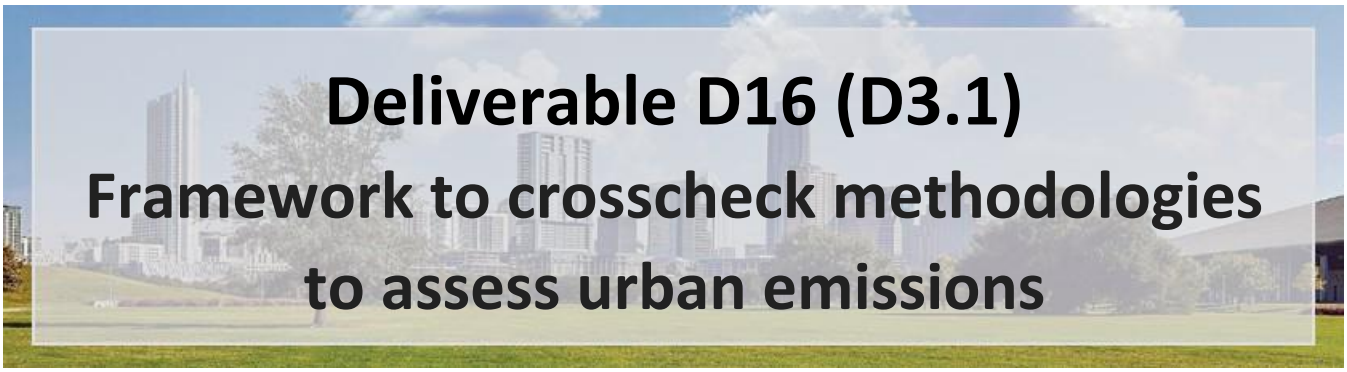

Deliverable D16 (D3.1)
Framework to crosscheck methodologies to assess urban emissions

RI-URBANS
Research Infrastructures Services Reinforcing Air Quality Monitoring Capacities in European Urban & Industrial AreaS (GA n. 101036245)

By

UHEL, BSC, CNRS, ENPC, FMI & KNMI

15 March 2024

RI-URBANS (www.RIURBANS.eu) is supported by the European Commission under the Horizon 2020 – Research and Innovation Framework Programme, H2020-GD-2020, Grant Agreement number: 101036245

Deliverable D16 (D3.1): Framework to cross-check methodologies to assess urban emissions

Authors: Leena Järvi (UHEL), Arnoud Apituley (KNMI), Marc Guevara (BSC), Oriol Jorba (BSC), Ari Karppinen (FMI), Rostislav Kouznetsov (FMI), Lya Lugon (ENPC), Jan Mateu (BSC), Soo-Jin Park (ENPC), Karine Sartelet (CNRS)

Work package (WP)	WP3 Improving modelling and emission inventories for policy assessment using advanced observation-based methodologies
Deliverable	D16 (D3.1)
Lead beneficiary	UHEL
Deliverable type	■ R (document, report) ☐ DEC (websites, patent filings, videos,….) ☐ Other: ORDP (open research data pilot)
Dissemination level	■ PU (public) ☐ CO (confidential, only members of consortium and European Commission))
Estimated delivery deadline	M30 (31/03/2024)
Actual delivery deadline	15/03/2024
Version	Final
Reviewed by	WP3 leaders and the project coordinators
Accepted by	Project coordination team
Comments	This report shows the results of the comparison of and crosschecking of methodologies to assess urban emissions and air quality and examine the improvements finer scale simulations can bring in specific case studies made in Barcelona (Spain), Paris (France), Turku (Finland), Helsinki (Finland) and Rotterdam (the Netherlands).

RI-URBANS (www.RIURBANS.eu) is supported by the European Commission under the Horizon 2020 – Research and Innovation Framework Programme, H2020-GD-2020, Grant Agreement number: 101036245

Table of Contents

RI-URBANS (www.RIURBANS.eu) is supported by the European Commission under the Horizon 2020 – Research and Innovation Framework Programme, H2020-GD-2020, Grant Agreement number: 101036245

1. About this document

One of the main objectives of WP3 is to better quantify emissions of gaseous and particulate pollutants at spatial-temporal scales relevant to urban areas (T3.1). Improved quantification is needed as the traditionally used mesoscale air quality models can reproduce the urban background conditions well, but are not able to solve air pollutant distributions, their dispersion and source-apportionment at resolutions needed for street-scale level within urban areas. To improve our understanding on urban emissions and dispersion, finer resolution models are needed to complement the traditionally used mesoscale air quality models. In T3.1 of WP3 we utilize multiple models to examine the enhancement of fine scale models would bring on examining urban emissions and air quality distributions. These include the PALM model system (Maronga et al., 2020), SILAM (System for Integrated modelling of Atmospheric Composition), street-network model MUNICH (Lugon et al. 2021, Kim et al. 2022), the CALIOPE-Urban multi-scale model (Benavides et al., 2019) and CAMS21b. The purpose of this document is to compare and crosscheck methodologies to assess urban emissions and air quality and examine the improvements finer scale simulations can bring in specific case studies made in Barcelona (Spain), Paris (France), Turku (Finland), Helsinki (Finland) and Rotterdam (the Netherlands). The PALM large-eddy simulations link ICOS and RI-URBANS.

For realistic simulation and quantification of gaseous and particulate pollutant emissions at high spatial and temporal resolution within urban neighbourhoods, detailed descriptions of model boundary conditions such as emissions and mesoscale forcing, and atmospheric processes relevant for pollutant dispersion are needed. In Barcelona, uncertainties and sensitivities associated with emission inventories aiming to identify the relevant sources impacting the urban background black carbon (BC) levels were studied by examining European-wide downscaled and bottom-up emission inventories. Major differences were found in the temporal disaggregation, spatial distribution and the Elemental/Organic Carbon (EC/OC) speciation assumed in each inventory. This demonstrates the importance of emission inventory in determining background concentrations needed also for realistic description on air quality and related dispersion within urban neighbourhoods. Similarly in Paris, we assessed the representation of traffic emissions by particularly focusing on comparing the impact of bottom-up and top-down traffic emission inventories. It was found how $PM_{2.5}$ concentrations are less sensitive to the inventory approach whereas better model performance was seen with bottom-up emission inventory for NO_2 and EC when compared against observations from urban background stations. For particle number concentrations (PNC), top-down inventory provides slightly better results than the bottom-up. This demonstrates the importance on considering multiple aerosol metrics when different methodologies to quantify urban emissions are compared.

We also studied the horizontal street-level dispersion and BC concentrations in Barcelona and how to reduce uncertainties in simulated fields and found how using localized meteorological information improved the local scale simulated BC concentrations. By using microscale traffic simulators and emission models we can better represent the impact of stop-and-go congestion on traffic emissions, improve the road-link emission estimations and furthermore the modelled concentrations. In Helsinki, we extended the examination of uncertainties concerning street-scale aerosol particles concentrations to examine the importance of introducing radiation interaction and aerosol particle dynamic processes in street-scale Large-Eddy Simulation (LES). In low wind speed condition, introduction of radiation interaction has a

RI-URBANS (www.RIURBANS.eu) is supported by the European Commission under the Horizon 2020 – Research and Innovation Framework Programme, H2020-GD-2020, Grant Agreement number: 101036245

major impact and can be one of the reasons why the local meteorological wind also improved the simulations in Barcelona as the thermal effects would not be included into the mesoscale model inputs whereas in local flow fields yes. The inclusion of aerosol particle processes was less important than radiation interaction on street-level concentrations, but still improved the modelling capabilities of the used LES model PALM. Running full aerosol-chemistry model in LES is however computationally expensive and thus we have also taken the first steps on providing LES-driven air quality forecasts where we combine high resolution flow from LES to a mesoscale air quality simulation allowing higher spatial and temporal resolution forecasts than traditional mesoscale models.

We also propose a toolbox for model evaluations over urban areas over the routine validation activity of the Copernicus Atmosphere Monitoring Service (CAMS) which would allow to study the added value of above-surface observations which are currently not exploited in an operational way, provide a link between in-situ surface and satellite column observations by using profile observations and exploit campaign data to better understand the three-dimensional distribution of pollutants.

The results from the different cities and activities demonstrate the first steps on producing a framework to cross-check methodologies and to improve the modelling capabilities of urban emissions and air quality distributions by producing new knowledge on the impact of chosen emission inventory on both background and urban air quality and on the processes needed to enhance street-level air quality modelling within urban areas.

This is a public document, available in the RI-URBANS website (https://riurbans.eu/work-package-3/#deliverables-wp3). The document will be distributed to all RI-URBANS partners for their use and submitted to European Commission as the RI-URBANS deliverable D16 (D3.1).

2. Enhancing air quality modelling capabilities in Barcelona

This section presents the results of two modelling exercises performed in the urban area of Barcelona to assess urban background and urban traffic BC levels. Mesoscale and urban scale modelling techniques were combined with observational data to assess the variability, source apportionment and uncertainties in emissions contributing to BC levels in the city of Barcelona. The modelling approach adopted combines results derived from both mesoscale air quality models (i.e. Multiscale Online Nonhydrostatic Atmosphere Chemistry, MONARCH, model; Badia et al., 2017) and street-scale urban dispersion models (the Operational Air Quality Forecast System for Spain, CALIOPE-urban model; Benavides et al., 2019). The following subsections present the work done and the main results. The two studies highlight the benefits of combining new observational datasets and modelling techniques to refine emission inventories and better understand and mitigate air pollution impacts in urban environments. The results of the first study were recently published in Navarro-Barboza et al. (2024).

2.1 Uncertainties in source apportionment of urban background air quality

Urban air quality is characterized by high spatio-temporal variability, mainly explained by urban background conditions and enhancements in street canyons attributed to local emissions (i.e. traffic). A first step towards accurately representing urban air quality in models relies on the precise description of background conditions, both in terms of emissions and dispersion. Here, we discuss the uncertainties and sensitivities associated with emission inventories, aiming to identify relevant sources impacting the urban background air quality of the Barcelona city.

RI-URBANS (www.RIURBANS.eu) is supported by the European Commission under the Horizon 2020 – Research and Innovation Framework Programme, H2020-GD-2020, Grant Agreement number: 101036245

We used the MONARCH model (Badia et al., 2017, Navarro-Barboza et al., 2024) and three different emission inventories - two versions of the European-scale emission inventory CAMS-REG (Kuenen et al., 2022) developed under CAMS and the High Elective Resolution Emission Systes (HERMESv3) detailed national inventory for Spain (Guevara et al., 2020) - to assess the uncertainties in BC simulation and source allocation (from traffic, residential wood combustion - RWC, shipping, fires and others) in the urban area of Barcelona. For this, measurements and source apportionment of BC gathered in WP1 performed by CSIC at a supersite representing an urban background environment were used in this work. The station is located within the Barcelona metropolitan area of nearly 4.5 million inhabitants (41º23'24'' 02º6'58'') at about 25 km from the coast, and at 200 m distance from one of the busiest streets in the city (> 60 k vehicles per day). BC concentrations were determined with Multi Angle Absorption Photometers (MAAP, Petzold and Schönlinner, 2004). The eBC concentrations were calculated by the MAAP's software using a local mass absorption cross section (MAC) value of 9.6 ± 3.2 m^2 g^{-1} calculated by comparing the absorption measurements provided by the MAAP with the EC concentrations obtained with a semi-continuous (3 h resolution) SUNSET analyser in the Barcelona station (Yus-Díez et al., 2022). The source contribution of BC was derived applying the Sandradewi et al. (2008) method to the absorption measurements performed with an AE33 aethalometer.

Table 1 summarises the main characteristics of the three emission inventories. The CAMS-REG_v4.2 (CRV42) has been built using the official emission data reported by each European country for each source category to the Convention on Long-Range Transboundary Air Pollution (CLRTAP) and the European Union National Emission Ceilings Directive. Emissions are given for different sectors using the Gridded Nomenclature For Reporting (GNFR) sectorization. The raw emission inventory maintains a consistent spatial resolution of 0.1°x0.05° (approximately 11 x 6 km^2) throughout Europe. It was released in 2020 providing emissions for an 18-year time series (2000–2017) consistently. The CRV42 inventory reports total annual emissions, and hourly emissions are derived through the application of temporal profiles (i.e., monthly, weekly and diurnal) per GNFR sector based on Denier van der Gon et al. (2011). Additionally, speciation profiles for PM (EC, OC) are provided per GNFR sector, country and year. As a complementary dataset, the CAMS-REG_v4.2-Ref2 (CRV42_REF2) is a science version of CRV42 using a consistent approach for RWC PM emissions. PM emissions (PM2.5 and PM10) from GNFR_C (other stationary combustion) were replaced with a bottom-up estimate (Denier Van Der Gon et al., 2015, Kuenen et al., 2022). This bottom-up approach considers activity data (wood usage and appliance types), consistent emission factors across Europe for RWC, including condensable fraction, for both wood and solid fuels, and spatial distribution based on population density and own wood consumption map. Besides GNFR_C sector, CRV42_REF2 incorporates the other sectors as present in CRV42. Speciation profiles for PM from GNFR_C are adjusted to reflect the inclusion of condensables in the total emissions. The third inventory is the Spanish emission inventory computed using the HERMESv3 bottom-up emission model (Hv3_BU) designed to provide bottom-up emissions from point sources (energy and manufacturing industries), road transport, residential and commercial combustion, other mobile sources, use of solvent and agricultural activities (livestock and use of fertilizers). A comprehensive compilation of activity data from multiple sources of information is combined along with emission factors based on EMEP/EEA emission inventory guidelines and meteorology information to derive final gridded emission estimates at hourly resolution. For the residential sector, Hv3_BU considers the condensable fraction of RWC PM, as reported in the EMEP/EEA emission inventory guidelines. Regarding RWC emissions, the three datasets consider the inclusion of condensable fraction in Spain, although CRV42 drags the inconsistency among different countries. One of the major differences between them is how RWC PM emissions are speciated (Table 1). The addition of condensable fraction implies an increase of OC mass emitted while EC should not be affected. Therefore, the speciation of EC/OC changes significantly from a 48.6/40.6% of the total PM2.5 in CRV42 (which neglects condensables in the speciation) to 9.8/87.7 and 7/75% in CRV42_REF2 and Hv3_BU, respectively. Remarkably, this results in an unexpected decrease in EC emissions for CRV42_REF2 in contrast to CRV42 in Spain, essentially rectifying the inconsistency inherent in CRV42.

RI-URBANS (www.RIURBANS.eu) is supported by the European Commission under the Horizon 2020 – Research and Innovation Framework Programme, H2020-GD-2020, Grant Agreement number: 101036245

Table 1. *Main characteristics of the three emission inventories used in this study.*

	CRV42	CRV42_REF2	Hv3_BU
Air pollutants	NOx, SO_2, NMVOC, NH_3,CO,PM_{10},$PM_{2.5}$	NOx, SO_2, NMVOC,NH_3,CO, PM_{10},$PM_{2.5}$	NOx, SO_2, NMVOC, NH_3,CO,PM_{10},$PM_{2.5}$
Reference year	2017	2017	2018
Domain	Europe	Europe	Spain
Spatial resolution	0.1x0.05deg	0.1x0.05deg	User configurable (5–1 km)
Temporal resolution	Yearly	Yearly	Hourly
condensable fraction RWC	Not consistently	Yes	Yes
EC fraction RWC[a]	0.4866	0.0989	0.07
OC fraction RWC[a]	0.4068	0.8778	0.75[b]
Reference	Kuenen et al., 2022	Denier Van Der Gon et al., 2015, Kuenen et al., 2022	Guevara et al., 2020

a RWC EC/OC speciation for Spain as reported by Kuenen et al., 2022

b Emissions compute organic mass and assumes OM:OC of 1.8 for RWC and 1.4 for other sources, as suggested by Klimont et al., 2017

Figure 1 shows the spatial distribution of RWC $PM_{2.5}$ emissions of CRV42_REF2 and Hv3_BU over a gridded domain at 5 km horizontal resolution. While CRV42_REF2 inventory shows a distribution of RWC towards urban areas, Hv3_BU methodology assigns them more in rural regions. In both CRV42 and CRV42_REF2, RWC emissions are spatially distributed using a specific European proxy that considers population density, degree of urbanisation and proximity to wood (Kuenen et al., 2022). The resulting spatial pattern principally follows population distribution but is also influenced by local wood availability. On the other hand, Hv3_BU combines the fuel statistic consumption of the residential sector at NUTS level 3 with the Global Human Settlement Layer (GHSL) population density and settlement category (urban, rural) data (Florczyk et al., 2019) to spatially allocate residential emissions. The use of biomass fuel for residential heating is not a common practice in cities across Spain and the total population density as a proxy to distribute RWC in the country may introduce bias in modelling results as will be shown later.

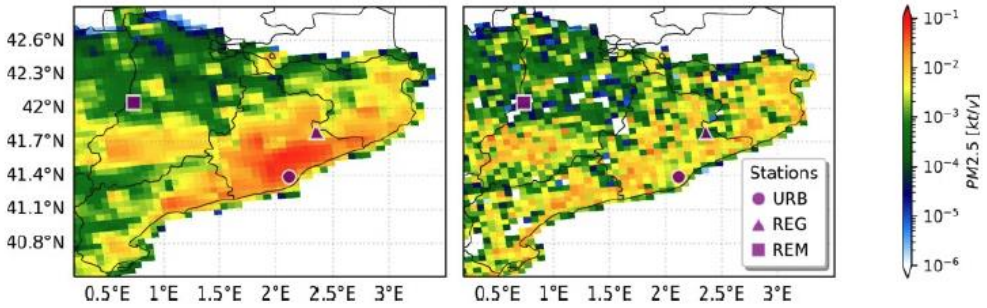

Figure 1. *Annual $PM_{2.5}$ RWC emissions for NE Spain from CRV42_REF2 (left) and Hv3_BU (kt/y) (right) gridded at 5 km horizontal resolution. The URB symbol indicates the localization of the monitoring sites used in this work.*

When looking at the temporal distribution of EC and $PM_{2.5}$ emissions estimated by each of the three datasets, relevant methodological differences arise in the temporal disaggregation, the attribution to specific sectors, and the EC/OC speciation assumed. Figure 2 shows the monthly distribution of total anthropogenic emissions for $PM^{2.5}$ and EC for each emission inventory used. The emissions are split into residential, on-road traffic, and other sectors. For the residential and traffic categories, all three inventories consider the same emissions sources except for road transport resuspension, which is only estimated by Hv3_BU. Nevertheless, while resuspension is an important contributor to total primary PM_{10}, its contribution to $PM_{2.5}$ and primary BC emissions is very limited (Rodriguez-Rey

RI-URBANS (www.RIURBANS.eu) is supported by the European Commission under the Horizon 2020 – Research and Innovation Framework Programme, H2020-GD-2020, Grant Agreement number: 101036245

et al., 2021). The CAMS inventories follow a V-shape seasonality, dominated by the residential sector, in $PM_{2.5}$ and EC. Specifically, residential emissions peak during wintertime while traffic and others are rather constant throughout the year. On the other hand, Hv3_BU uses specific profiles per sector with relevant differences compared with the previous ones. For residential emissions a day-of-year time distribution based on the heating degree-day approach (Guevara et al., 2021) is used. In the case of road transport emissions, the seasonality of Hv3_BU emissions is derived from observed traffic count datasets. This results in residential emissions peaking in February, which is likely related to the cold spell felt throughout Europe during February 2018 (Copernicus 2018), and traffic emissions showing a clear reduction during August in Barcelona, when people are away for holidays. Major differences are found in the distribution of total emissions per sector. While Hv3_BU suggests that traffic is the dominant source of $PM_{2.5}$ and BC emissions in the city of Barcelona, both CRV42 and CRV42_REF2 assign a larger share of these emissions to the residential sector. Specifically, on an annual basis, CRV42 assigns 50.2% to the residential sector and 10.2% to traffic, while CRV42_REF2 assigns 57.5% to the residential sector and 8.8% to traffic. In contrast, Hv3_BU accounts for 12.9% of $PM_{2.5}$ emissions in the residential sector and 72% in traffic for Barcelona. The discrepancies in source contributions observed here are in line with the results found in the emission intercomparison exercise performed in Task 3.2, which revealed that CAMS emission inventories tend to under allocate road transport emissions in urban areas when compared to local bottom-up inventories (see Milestone M3.3 report for more details).

Finally, the treatment of condensable fraction in the residential sector introduces another source of relevant differences between CRV42 and the other two inventories. While the residential $PM_{2.5}$ emissions are rather consistent in both CAMS inventories, the speciation used to derive EC/OC emissions (Table 1) reduces EC emissions around a factor of four in the CRV42_REF2 compared with CRV42. This discrepancy is because in CRV42 the speciation proposed for RWC assumes that condensable compounds are not included in the national emissions used as input in the CAMS inventory. Nevertheless, in the case of Spain the condensable fraction is considered in official reported emissions (Fagerli et al., 2019) and subsequently in the CRV42 inventory.

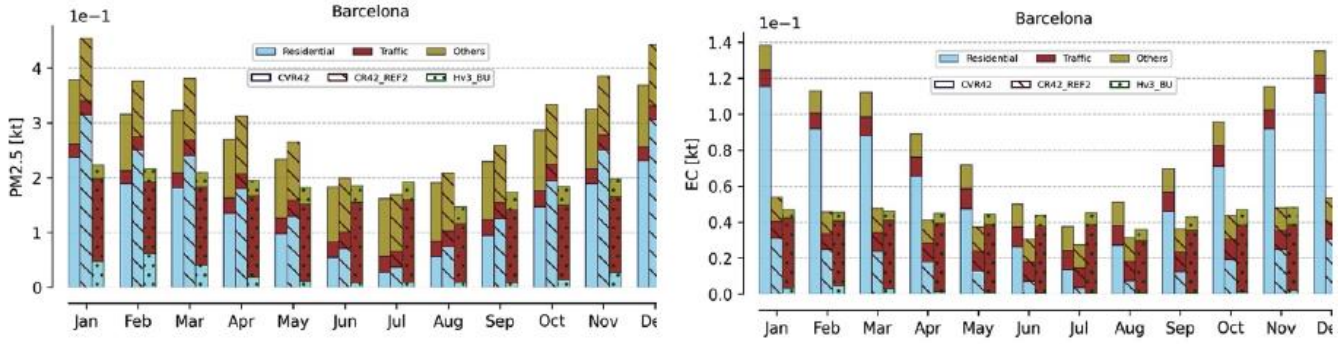

Figure 2. *Monthly anthropogenic emissions of fine particulate matter ($PM_{2.5}$, left) and elemental carbon (EC, right) derived from CRV42, CRV42_REF2 and Hv3_BU inventories over the city of Barcelona. Emissions are split in residential sector (light-blue), on-road traffic emissions (red), and the remaining as other emissions (dark-gold).*

The way the fraction of condensable material is included in RWC emissions strongly impacts the results of the MONARCH chemistry model. Figure 3 shows the monthly average surface concentration of BC at the Barcelona urban background site simulated by the model at ~5 km horizontal resolution using the three emission inventories described above. Run-1 (using CRV42 emissions) shows a systematic overestimation during wintertime, meanwhile Run-2 (using CRV42_REF2) and Run-3 (using Hv3_BU) results capture reasonably well the monthly variability and concentrations of BC. Overall, the treatment of RWC emissions in Run-2 and Run-3 are more consistent with observations. The main differences with Run-1 can be explained by the important change in the speciation profile (see Table 1) more than by a possible change in total $PM_{2.5}$ emissions reported by the inventories for Spain (Figure

RI-URBANS (www.RIURBANS.eu) is supported by the European Commission under the Horizon 2020 – Research and Innovation Framework Programme, H2020-GD-2020, Grant Agreement number: 101036245

2). It is also worth mentioning the role of temporal disaggregation of emissions used in the different inventories. For instance, observations show an increase in BC concentrations from January to February in 2018, a feature captured by Hv3_BU and not by the CAMS inventories mainly due to the specific methodologies used in the different datasets, as discussed above.

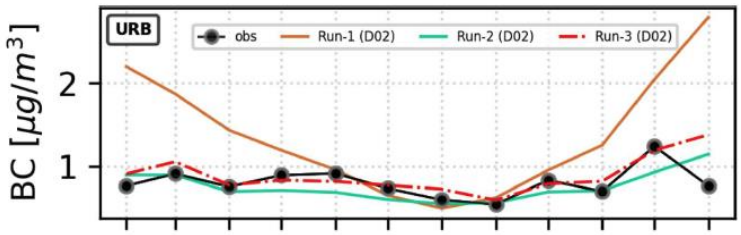

Figure 3. *Monthly mean observed (black line) and modelled surface concentrations of BC at the Barcelona urban background site using three emission inventories (CRV42 orange line, CRV42_REF2 cyan line, and Hv3_BU dash-dotted red line) for 2018. Results of D02 at 5km horizontal resolution.*

To understand how different emission sectors contribute to BC concentrations, we have run the MONARCH model tagging the contributions from the residential, traffic, shipping, fires (biomass burning) and other emission sources. Figure 4 provides a synthesis of the monthly mean contribution (absolute values and percentage) of BC emission sources to surface concentrations derived from observations and model results, for January and July respectively, at the Barcelona urban background site. The first column of the figure presents the contribution of fossil and non-fossil contributions as derived from WP1 observations. The fossil contribution represents the contribution to the measured BC concentrations from fossil fuel combustion sources (mainly dominated by traffic, and to a lesser extent by other sources like shipping, industries and power generation; natural gas can be also considered a fossil source of BC), and non-fossil describes other than fossil BC sources from combustion of non-fossil fuel like biomass burning and agricultural waste burning. The second column presents the model contribution of different sectors, such as traffic, residential, fires, shipping, and others, using the CRV42_REF2 emission inventory. Finally, the third column presents the corresponding results using Hv3_BU emissions. The fossil contribution reported by observations represents the contribution to the measured BC concentrations from fossil fuel combustion sources (mainly dominated by traffic, and to a lesser extent by other sources like shipping, industries and power generation), while the non-fossil fuel contribution describes other than fossil BC sources from combustion of non-fossil fuel like biomass burning and agricultural waste burning. There is no direct equivalence between the fossil/non-fossil contribution quantified by observations and the model tags used here. We consider that the fossil contribution derived from observations is closely related to traffic tag plus shipping tag plus others tag of the model. On the other hand, non-fossil sources in the model tags are mainly considered by residential and fires tags. The comparison between model and measurements is used as an indication of how the model characterizes the main source contributions but has relevant uncertainties in both model and observational aspects.

The analysis of the model results reveals a significant under-representation of traffic in CRV42_REF2. Observed concentrations appears to be dominated by on-road traffic emissions which contribute significantly to the high observed fossil contribution in January (78.8%) and in July (84.2%). However, CRV42_REF2 model results underestimate traffic influence, with a contribution of only 18.5% in January and 25.8% in July. The under-representation of the observed fossil contribution by CRV42_REF2 remains in January even if we add the contribution from both shipping (19.5%) and others (4.6%) to traffic. However, it reduces significantly in July mainly due to the increased role of shipping (49.8%). Conversely, we find that the residential contribution is overestimated in January using CRV42_REF2 compared to observed non-fossil contribution of 21.2%. Again, much better agreement is identified in July (not just considering residential but fires). Regarding Hv3_BU emissions, our results

RI-URBANS (www.RIURBANS.eu) is supported by the European Commission under the Horizon 2020 – Research and Innovation Framework Programme, H2020-GD-2020, Grant Agreement number: 101036245

show good agreement with observations, with the fossil contribution to BC ranging from 70% to 80% in both January and July. This agreement is achieved by considering that mainly traffic plus shipping (76.5% and 79% in January and July) explain the observed fossil contribution (78.8% and 84.2%). Additionally, the agreement with observations improves if we consider that a fraction of others is a fossil source. While both CRV42_REF2 and Hv3_BU inventories show consistency in total PM emissions, as depicted in Figure 3, their sector contribution significantly differs. According to CRV42_REF2, the residential sector (56.7% in January) and the shipping sector (49.8% in July) are specifically responsible for a substantial amount of BC concentrations. However, Hv3_BU and observational data point to a stronger contribution from the traffic sector, estimated at 65–70%. The use of detailed databases for Spain within Hv3_BU contributes to the precision and refinement of the emission estimates. This granularity and detail in emission generation might be one of the key reasons behind the uncertainties observed in traffic, residential, and shipping emissions between CRV42_REF2 and Hv3_BU.

The results of the comparisons shown here highlight the advantages of using bottom-up approaches that incorporate specific information about a region, and the need to revise the spatial distribution of residential emissions in continental-scale inventories like CAMS-REG.

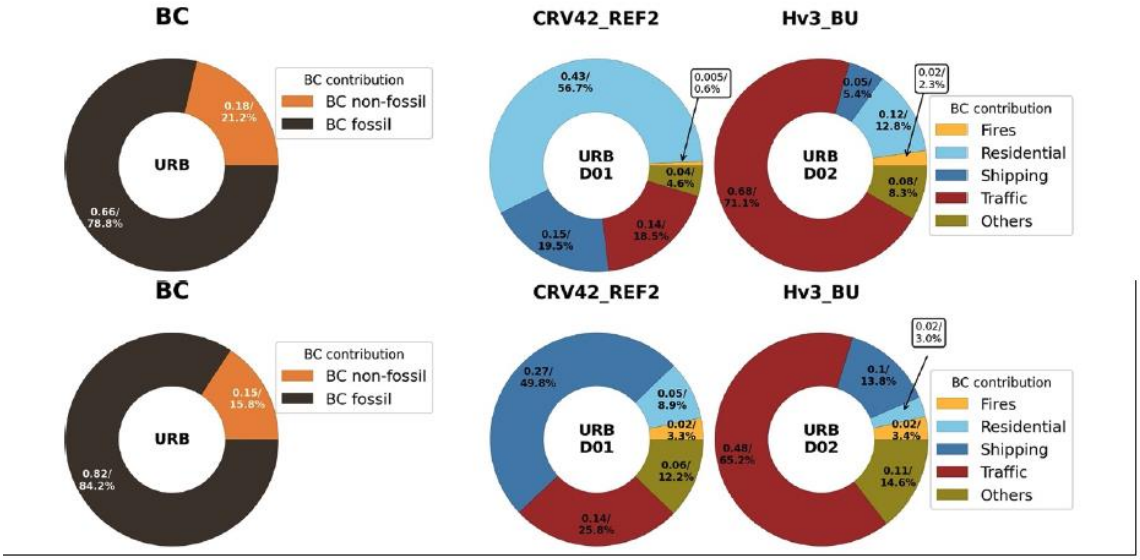

Figure 4. *The monthly mean contribution of BC surface concentration from emission sources for January and July 2018 at the Barcelona urban background station derived from (a) observations and (b) the MONARCH simulations using the CRV42_REF2 and Hv3_BU emissions. The colours indicate the different emission sources tagged. The labels on each sector of the pie chart show the contribution in both absolute value [ug m^{-3}] and percentage.*

2.2 Improved street-scale dispersion

In this section, we delve further into the uncertainties of urban emissions through a comprehensive analysis of street-scale dispersion modelling of BC in Barcelona city. The modelling tool used in the analysis is the CALIOPE-Urban air quality system (Benavides et al., 2019). CALIOPE-Urban estimates hourly concentrations of pollutants (NO_2, BC, $PM_{2.5}$) by coupling the results of a mesoscale air quality model (CMAQ or MONARCH), which provides background concentrations and meteorological data, with road-link traffic emissions and a Gaussian dispersion model adapted to street canyons. Here, the street-canyon dispersion of CALIOPE-Urban has been enhanced by introducing multiple reflections of the dispersion plume from the facades of the street-canyon buildings. Two reflections are used by default. The system was also updated by introducing a new submodule that allows modelling

RI-URBANS (www.RIURBANS.eu) is supported by the European Commission under the Horizon 2020 – Research and Innovation Framework Programme, H2020-GD-2020, Grant Agreement number: 101036245

the dispersion and concentration levels of BC, as the version described in Benavides et al. (2019) only covers NO_2. In the CALIOPE-Urban system, BC is treated as inert species, which experiences no chemical transformation within the timescale of concern (seconds to minutes). Because most BC occurs as sub-micron particles, they are expected to adopt the flow velocity very quickly (i.e., with small Stokes number), and it is reasonable to assume that they will disperse like gaseous species (Tong et al., 2012).

Figure 5 shows the annual mean BC concentrations estimated by the updated version of the CALIOPE-Urban system for the city of Barcelona at 20x20 m^2 resolution for 2019. Modelled results were compared against observations reported at an urban background site. A conversion from measured BC to eBC was performed considering a MAC value of 10 $m^2\ g^{-1}$, based on Yus-Díez et al. (2022). We also included the results of the CMAQ mesoscale model at 1x1 km^2 to illustrate the added value of the urban scale model, which allows to improve the reproduction of the morning peaks, especially during wintertime.

Results of the new version of the CALIOPE-Urban system are compared with a set of observed horizontal BC profiles measured in Barcelona city in 2015 (Amato et al., 2019). Our aim is to better understand the local dispersion of BC in different areas of the city and identify which are the key processes that explain the measured concentrations. For that, CALIOPE-Urban is used and different sensitivity runs are conducted perturbing meteorology and emissions following the methodology described in Benavides (2020) and briefly described below.

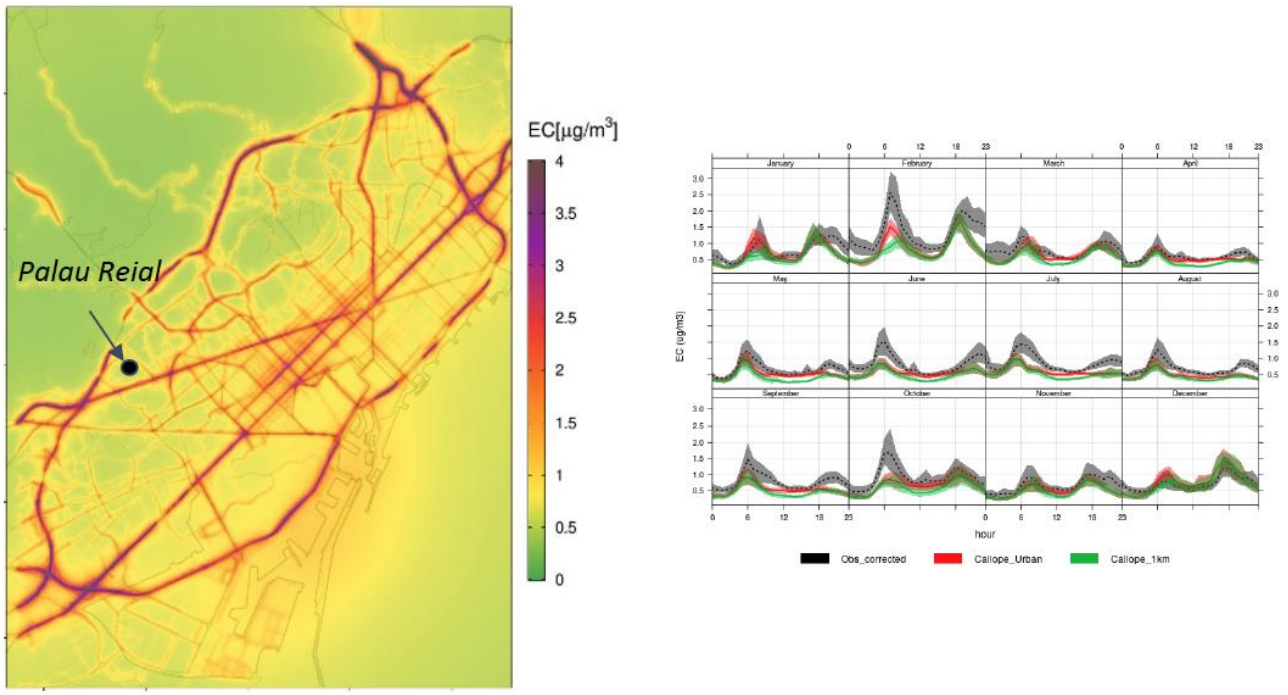

Figure 5. *Annual mean BC concentrations estimated by the updated CALIOPE-Urban system for the city of Barcelona at 20x20 m^2 resolution for the year 2019 (left) and comparison of the BC modelled results using the CALIOPE mesoscale (1x1 km^2) and CALIOPE-Urban systems (20mx20m) against measurements made at the urban background site of Palau Reial (right)*

BC horizontal profiles were measured using several AE-51 micro-aethalometers with a time resolution of 30 s spatially distributed (horizontal) to measure simultaneously the concentrations. The instruments were located starting on a road edge until a maximum distance of 250 m along pedestrian areas or at very low intensity traffic streets to avoid the interference of surrounding road sources. The measurements were conducted during 30 minutes between 9 am and 7 pm local time. Here, we consider the profiles measured in the open-road Diagonal

RI-URBANS (www.RIURBANS.eu) is supported by the European Commission under the Horizon 2020 – Research and Innovation Framework Programme, H2020-GD-2020, Grant Agreement number: 101036245

Street and at the Ciutadella urban park (Figure 6). In the first measurement location, the profiles were measured perpendicular to a very heavy traffic access road (i.e. annual average daily traffic equals 109 600 vehicles per day), while the second location represents a more urban background environment (the closest street to the measurements has an annual average daily traffic of 12 400 vehicles per day) (Amato et al., 2019). A conversion from measured BC to eBC is performed considering the same MAC value reported before (10 m2 g-1).

Figure 6. *Location of the measurements monitoring the horizontal dispersion of BC in Barcelona at Ciutadella park (left) and Diagonal avenue (right) used in this work.*

Freshly emitted particles from road traffic in the streets are estimated by the HERMESv3 bottom-up emission model at the hourly and road link level using the COPERT5 road transport exhaust emission factor database as reported in the EMEP/EEA emission inventory guidelines (Guevara et al., 2020). HERMESv3 also estimates non-exhaust PM traffic emissions, including road-surface, tyre and brake wear and resuspension. Specific speciation profiles are used to derive BC from the total PM estimated emissions. For exhaust and wear emissions, the vehicle and process-dependent profiles reported by the EMEP/EEA guidelines are used, while for resuspension emissions we consider the composition measured by Amato et al. (2012).

Figure 7 shows the average BC horizontal profiles reported by the observations and the CALIOPE-Urban system at the Diagonal Av. and the Ciutadella urban park measurement locations. In the observations, we see a deep fall-off on the horizontal dispersion profiles within the initial 5-10 m. CALIOPE-Urban follows the main dynamic observed in BC concentrations, with higher concentrations near the road edge tending to lower levels at growing distances from the edge. The modelled results are in the order of magnitude of the observations (i.e. within a factor of 2), but with a significant underestimation. In Ciutadella urban park, the modelled initial fall-off is slightly underestimated, and the model tends to better agree with observations beyond 50 m distance from the road edge. On Diagonal street the modelled initial fall-off is largely underestimated.

We hypothesize that the inputs of meteorological fields and road-link emissions may explain some of the discrepancies found between model results and observations. To further investigate that, two sensitivity test runs were performed with CALIOPE-Urban following Benavides (2020). In the first one, we replaced the wind speed and direction and PBL height of the mesoscale model used as input by observations derived from a meteorological station located on a building roof in Barcelona. We could not replace any of the turbulent parameters considered in the system because measurements are not available. Although the winds measured by the meteorological station may not be completely representative of the winds over the entire city, it provides a good indication of sensitivity of the model to the meteorological input parameters. As shown in Figure 7, the use of observational-based winds allows improvement in the model performance in reproducing the horizontal profile measured at the Ciutadella urban park, with the model being able to reproduce the high BC concentrations observed in the 0-5 m from the traffic street (concentrations increasing from approximately 5250 to 6750 $ng \cdot m^{-3}$). On the contrary, the meteorological impact on modelled results at the Diagonal Street does not explain the bias within the first meters.

RI-URBANS (www.RIURBANS.eu) is supported by the European Commission under the Horizon 2020 – Research and Innovation Framework Programme, H2020-GD-2020, Grant Agreement number: 101036245

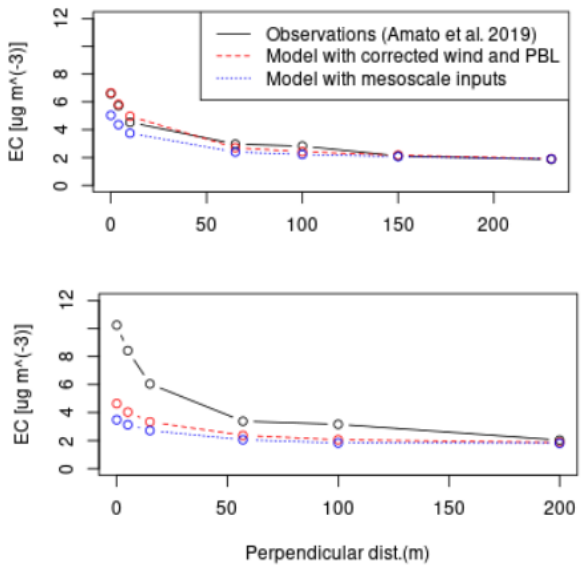

Figure 7. *Horizontal profiles of BC dispersion simulated by CALIOPE-Urban (colour lines) and measured (black line) in Ciutadella (top) and Diagonal (bottom) locations.*

Considering that traffic activity is larger in the Diagonal Av., we hypothesize that modifying road traffic emissions could potentially improve the model performance, mainly within the initial 0-10 m. This hypothesis is based on the fact that HERMESv3 estimates hourly road traffic emissions using the average speed model COPERT 5, which cannot account for particular congested situations of interest. The limitation of reflecting the increase in emissions due to stop-and-go conditions has been studied in previous works (e.g., Rodríguez-Rey et al., 2021). Since horizontal profile measurements were gathered during periods of 20-30 min, we may be missing details in the emissions due to the use of hourly modelled data. To overcome this limitation, we used the independent estimation of traffic emissions described in Benavides (2020) combining a microscopic traffic simulation model (AIMSUM Next AIMSUN, 2019) with an instantaneous vehicle emission model (PHEMLight; TUG, 2017).

First, the vehicle movement is derived from AIMSUM, which records the position and speed of each vehicle at a time step of 1 s. AIMSUN employs stochastic traffic assignment and default parameters for cars and buses typologies. Resulting vehicle speeds are then inputted into the microscopic vehicle emission model PHEMLight. PHEMLight uses the estimated vehicle's driving pattern and vehicle characteristics data to calculate instantaneous values of engine power and engine speed (i.e. 1 s). These values are then used to determine the associated emission factors (Hausberger et al., 2009). Finally, exhaust emissions are computed based on vehicle-specific power with 1 s temporal resolution, using a vehicle type categorization based on the Barcelona vehicle fleet composition profile from HERMESv3. Emissions for each street segment surrounding the Diagonal Street location are aggregated at high temporal resolution (i.e. 1 min and 1 hour). Figure 8a shows a comparison between the hourly PM_{10} exhaust emissions computed with HERMESv3 and PHEMLight at the Diagonal street location. The grey and yellow lines represent the hourly traffic flow considered in each model, the values being very consistent. PHEMLight emissions are greater than HERMESv3 emissions, especially during rush hours. The influence of considering the congestion in traffic (acceleration/deceleration and traffic lights) in PHEMLight can explain the main differences found when compared to HERMESv3. Figure 8b shows minute emissions estimated at 10:00 UTC using PHEMLight characterized by a large temporal variability. This results in a higher value of the hourly average emissions when compared to HERMESv3 results. The large variation in emission fluxes is mainly a consequence of the traffic light located in this street, which increases the number of vehicles in start-stop driving pattern.

RI-URBANS (www.RIURBANS.eu) is supported by the European Commission under the Horizon 2020 – Research and Innovation Framework Programme, H2020-GD-2020, Grant Agreement number: 101036245

We derived emission scaling factors from the intra-hourly variability estimated with PHEMLight (Figure 8b) and used them to scale the original HERMESv3 emissions. The scaling factors (0.56 and 2) were computed by dividing the maximum/minimum PHEMLight instantaneous emissions by the hourly average HERMESv3 estimated emissions. Figure 9 shows the impact on BC modelled concentrations of perturbing the emissions on the nearest street segments to the Diagonal street measurement location. The nearest street segments contribute more to the initial 0-10 m, where the model clearly underestimates BC concentrations. Results indicate that the model is very sensitive to the emission variability derived from the results calculated combining AIMSUN and PHEMLight. We see that when applying the upper scaling factor (2) the modelled BC concentrations within the initial 50 m are in line with the observations (increase from approximately 4750 to 7900 ng m^{-3}), the initial fall off also being better reproduced.

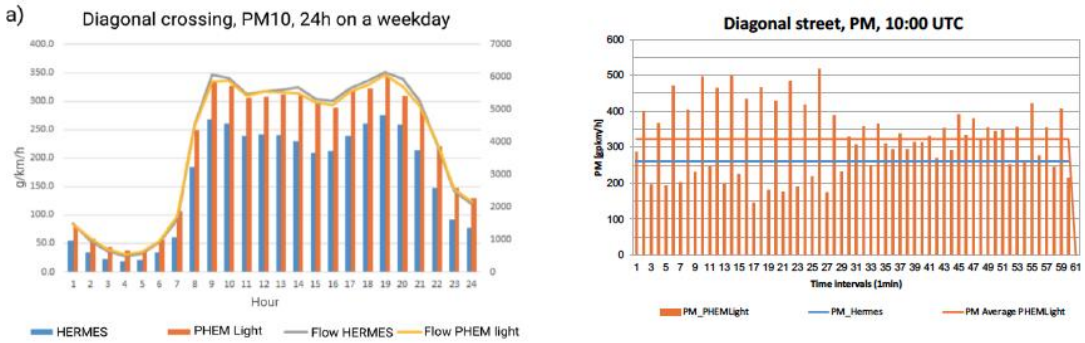

***Figure 8**. PM_{10} exhaust emissions (g km^{-1} h^{-1}) estimated with HERMESv3 and PHEMLight in Diagonal street. The top plot shows comparison between hourly emissions in UTC (left axis) and traffic flow intensity (right axis) estimated by both models, while the bottom plot compares the PHEMLight minutely emissions at 10:00 UTC (vertical bars) with the hourly mean value estimated by both HERMESv3 and PHEMLight (horizontal lines). For emissions, orange colour depicts PHEMLight and blue is HERMESv3. For traffic flow, yellow is PHEMLight and grey is HERMESv3.*

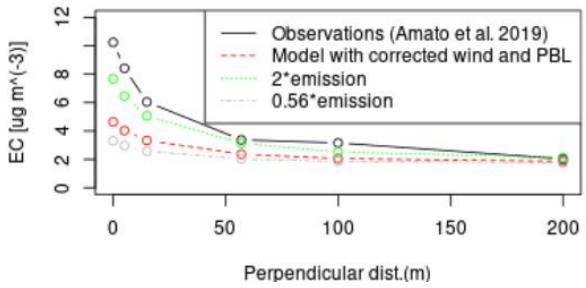

***Figure 9.** Horizontal profiles of BC dispersion simulated by CALIOPE-Urban (colour lines) and measured (black line) in Diagonal location perturbing traffic emissions with 0.56 and 2 factors.*

Results from this exercise indicate how the consideration of stop-and-go conditions in road transport emissions may explain part of the uncertainty in the modelling results, especially when measurements are averaged over periods below an hour and performed very close to the vehicles' tailpipes. Extrapolating this modelling approach to an entire city is, however, challenging as it would require setting up and calibrate microscale traffic simulator for the entire city. Therefore, such modelling approaches should be limited to hotspots urban regions, where air quality levels tend to present exceedances. Despite scaling up the emissions and adjusting meteorology according to observations, the model still fails to completely capture the steep increase in concentration near the main traffic lane (i.e., first 5-10m), which may indicate other uncertainties related to road transport emissions. This uncertainty could be related to missing processes in the considered emission factors, such as Diesel particulate filters (DPFs) malfunctions and tampering, which can significantly increase diesel cars PM emissions (e.g., Giechaskiel et al. 2022).

RI-URBANS (www.RIURBANS.eu) is supported by the European Commission under the Horizon 2020 – Research and Innovation Framework Programme, H2020-GD-2020, Grant Agreement number: 101036245

Real world measurements should be performed to quantify which fraction of the circulating vehicles may be affected by the aforementioned issues, so that local adjustments to the emission factors databases can be performed (e.g., Bernard et al. 2021).

3. MUNICH model to estimate accuracy of traffic emission factors from modelled concentrations

Concentrations are simulated in the streets of Paris using the street-network model MUNICH (Lugon et al., 2021, Kim et al., 2022). Comparisons to concentrations at traffic stations may allow us to assess the representation of traffic emissions in the model. Concentrations in streets are strongly influenced by traffic emissions, but also by the urban background concentrations, which evolve depending on all other emission sources. The urban background concentrations are simulated by the CHIMERE model (Menut et al., 2021) coupled to aerosol module SSH-aerosol (Sartelet et al., 2020). They are used as boundary conditions in the MUNICH simulations. As the same chemistry and aerosol module is used at the regional scale and in the street network, the representation of chemistry and aerosol dynamics is coherent at all scales, from the street to the background. At the regional scale, the domain of simulation is discretized with a 1x1 km^2 resolution and a zoom is performed down to the streets of Paris.

As BC and PNC are strongly influenced by traffic, a bottom-up approach is used for emissions. The road traffic emissions data were produced by Airparif based on the results obtained using the Heaven system originally developed in 2001 as part of the European project of the same name in partnership with the road traffic management departments of the City of Paris and the Direction Régionale de l'Equipement d'Ile-de-France. Since then, this system has been regularly updated on all its components: emission factors, vehicle fleets, traffic model, real-time countings, network, etc., to have the most recent information on vehicle emissions in the Paris region. The strength of this system is to use a traffic model that is corrected from the count data received in near-real time. In the chain CHIMERE/MUNICH, the regional-scale traffic emissions were estimated by aggregating the local-scale emissions corrected from the local traffic counts. For other activity sectors, the Aiparif inventory of 2019 was used. PN emissions were estimated from the Airparif inventory using methodology from Sartelet et al. (2022).

To assess the influence of the representation of emissions, regional-scale simulations were also performed using the top-down emission inventory EMEP during two months in June and July 2022. For comparisons to observations, as the model simulates EC, the BC observed concentrations are normalized using a harmonization factor, following Savadkoohi et al. (2023). A harmonization factor of 1.7 was determined for Paris in the summer 2022 using EC and BC collocated measurements at Les Halles station, which is an urban background station operated by Airparif in the center of Paris.

The measured and simulated concentrations are compared in Table 2 at urban background stations and traffic stations for NO_2, $PM_{2.5}$, EC and PNC. For all pollutants and at all station types, the mean concentrations compare well to the observations satisfying the model performance criteria (MFE < 75%, MFB < ±50%) and the model performance goal (MFE< 50% and MFB < ±30%) of Boylan and Russell (2006). The model represents well the concentrations of NO_2, $PM_{2.5}$, EC and PNC at traffic stations, suggesting that the traffic emissions are well modelled, and that the traffic emission factors used are appropriate. To build the inventory, COPERT emission factors described in the EMEP/EEA air pollutant emission inventory guidebook were used for NO_x and PM. The NO_x speciation was determined using the COPERT ratio NO_2/NO_x that depends on vehicle types, and the speciation of PM exhaust emission factors also follows the COPERT methodology by using the fractions of BC and OM supplied for each vehicle type. The size distribution of traffic non-exhaust emissions was calculated using the NORTRIP model for $PM_{2.5}/PM_{10}$ (Denby et al., 2013) and EMEP guidelines for the $PM_1/PM_{2.5}$ ratio (Ntziachristos et al., 2013). For PN, emissions were estimated using ratio $PM_{2.5}/PM_1$ and $PM_1/PM_{0.1}$ and an algorithm that conserves mass and number for distributing $PM_{0.1}$ emissions in particle sizes.

RI-URBANS (www.RIURBANS.eu) is supported by the European Commission under the Horizon 2020 – Research and Innovation Framework Programme, H2020-GD-2020, Grant Agreement number: 101036245

Table 2: Comparisons of simulated and measured concentrations, MFE and MFB are the mean fractional error and the mean fractional bias respectively.

	Station type	Number of stations	Observed (µg m^{-3} for NO_2 and EC, # cm^{-3} for PNC)	Modelled (µg m^{-3} for NO_2 and EC, # cm^{-3} for PNC)	MFE (%)	MFB (%)
NO_2	Urban Airparif	21	15.0	15.6	34	5
	Urban EMEP	0.4	15.0	18.0	35	21
	Traffic	10	40.0	41	26	4
$PM_{2.5}$	Urban Airparif	8	7.2	8.3	33	21
	Urban EMEP	8	7.2	8.9	36	28
	Traffic	3	11.2	11.8	20	7
EC	Urban	4	0.4	0.4	50	0
	Urban EMEP	4	0.4	0.6	51	38
	Traffic	3	1.3	1.1	37	4
PNC	Urban	3	8145	5843	41	-34
	Urban EMEP	3	8145	6728	29	-19
	Traffic	1	9141	7713	23	-13

At urban background stations, comparisons between concentrations simulated with the top-down inventory EMEP and with the bottom-up inventory corrected by traffic loop counts show that NO_2 and EC are better simulated with the bottom-up inventory. Less differences between the two inventories are observed for $PM_{2.5}$, although the statistics of comparisons are slightly better using the bottom-up inventory. On the opposite, for PNC, the statistics are slightly better using the top-down inventory, but this is could be due to uncertainties in modelling PNC concentrations.

4. LES modelling of eddy fluxes and improved quantification of pollutant dispersion

One of the aims in T3.1 was to combine urban eddy covariance (Ec) measurements and high-resolution LES modelling to quantify the spatial and temporal dynamics of urban emission fluxes and thus improve the emission data products. While writing the project proposal, we were expecting that simulations with large enough computation domain needed to solve turbulence within the source area of the Ec measurements would be straightforward to conduct using the PALM model system. Our plan was to use three nested domains in such a way that we would resolve most turbulent eddies within the finest child domain with 2-3 m resolution and when moving to coarser parent and root domains, start to use parameterised land surface processes as directly resolving turbulence is not meaningful with grid resolutions of 8-12 m. However, during the project we realised that the module describing land surface interactions in PALM does not cover urban surfaces meaning that it is challenging

RI-URBANS (www.RIURBANS.eu) is supported by the European Commission under the Horizon 2020 – Research and Innovation Framework Programme, H2020-GD-2020, Grant Agreement number: 101036245

to produce realistic surface forcing in our model simulations. As a result, we started to implement an urban land surface model to the model system. This has resulted delays in our actual model simulations concerning comparisons with eddy fluxes.

Meanwhile we have, however, worked intensively to understand the relevant processes needed to conduct realistic turbulence simulations and air quality predictions within urban settings and complement the findings from Barcelona and Paris as described above. We have studied the impact of the inclusion of radiation interaction into a high-resolution LES as well as the importance of inclusion of aerosol particle dynamics into such simulation using the comprehensive PALM model system 6.0. The study was conducted in urban neighbourhood in Helsinki, Finland, through where one of the main roads leading to Helsinki city centre passes. On the road also one of the urban air-quality monitoring supersites operated by the Helsinki Region Environmental Services Authority is located and an intensive observation measurement campaign using a drone and mobile laboratory was conducted in 2017 to map the spatial variability of air pollutant concentrations (Järvi et al., 2023). The PALM model setup consisted of a root (768×768 cells, 9 m grid resolution), parent (768×768 cells, 3 m grid resolution) and child (576×576 cells, 1 m grid resolution) domains. The surface energy balance and flow were solved in each domain but the sectional aerosol module SALSA only in the child domain. Dynamic boundary conditions were obtained from the MetCoOp Ensemble Prediction System (MEPS), which provides the necessary forcing for initialising the large-scale motions in the atmosphere. The trajectory model for Aerosol Dynamics, gas and particle phase CHEMistry (ADCHEM; Roldin et al., 2011b) was used to give the background trace gas concentrations, particle number concentrations and chemical composition of aerosol particles for SALSA. Emissions from road traffic within the child domain were estimated by combining information on hourly vehicle fleet composition, and particle number and gaseous unit emissions factors. In SALSA the aerosol particle size distribution was described by 10 bins ranging from 2.5 nm to 1 µm, and the particles contained sulphate, organic carbon, black carbon, nitrate and ammonium. The aerosol processes of condensation, coagulation and dry deposition were included in the simulations. The rapid radiative transfer model for global model (RRTMG) and a separate multi-reflection radiation transfer model (RTM) were used to solve the energy balance over all surfaces and calculate radiation interaction within the child domain. We conducted a base run with both aerosol processes and radiation interaction off, runs where one of the processes was turned on and finally a run where both processes were turned on.

We found how inclusion of radiation interaction in LES is critical to produce realistic flow fields, dispersion and furthermore local air pollutant concentrations at least in low wind speed conditions (Figures 10, 11, Strömberg et al., 2023). The implementation of the radiation interaction increased near-surface temperatures by 44%, flow fields by 87% and the pedestrian-level (4 m) total particle number concentrations by 53 %. The importance of aerosol processes is less important but still significant. The impact of inclusion of dynamic aerosol processes in the simulation of total number concentrations were found to be 18%. In street-level aerosol particle simulations within dense urban neighbourhoods' dry deposition has been found to be the most important aerosol process over condensation, coagulation and evaporation (Kurppa et al., 2019). These results highlight uncertainties related to air pollutant simulations at the high temporal and spatial resolutions within urban neighbourhoods.

RI-URBANS (www.RIURBANS.eu) is supported by the European Commission under the Horizon 2020 – Research and Innovation Framework Programme, H2020-GD-2020, Grant Agreement number: 101036245

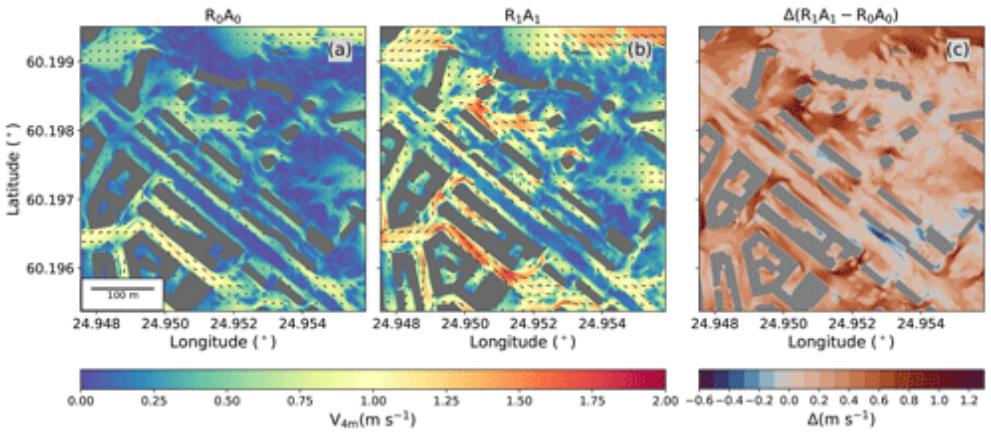

Figure 10. *The impact of radiation interaction on pedestrian level flow fields within urban neighbourhoods as simulated using the PALM model system (Strömberg et al., 2023). Flow field with a) the baseline simulation without radiation interaction, b) simulation with radiation interaction on and c) their difference.*

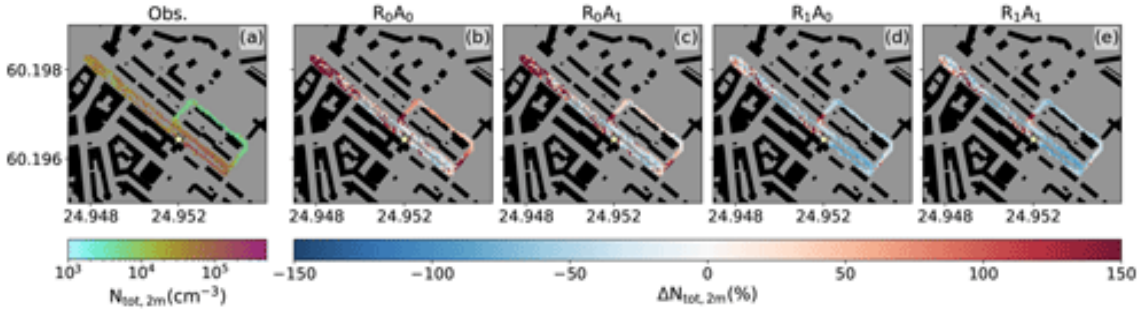

Figure 11. *Improvement in PALM model system performance in simulating aerosol particle number concentrations with the inclusion of radiation interaction and/or aerosol dynamic processes (Strömberg et al., 2023). The spatial variability of a) observed number concentrations as measured using a mobile laboratory, and difference between the observed and modelled concentrations when b) no radiation interaction and aerosol processes are included, c) aerosol processes are included, d) radiation interaction is included and e) both aerosol process and radiation interaction are included in the PALM model run.*

5. Towards offline LES-driven air-quality forecasts at urban scale

While LES models have been developed to incorporate chemical transformations, the utilization of LES in operational air-quality forecasting at an urban scale has proven to be computationally prohibitive. Therefore, an offline chemistry-transport model, SILAM (https://silam.fmi.fi), has been integrated with PALM LES, allowing for efficient offline computations of atmospheric chemistry at a city scale with deca-metric resolution.

In collaboration with the EU RESPONSE project, PALM model system has been employed to compute wind fields over the city of Turku corresponding to various directions of the synoptic wind. Under neutral stratification, the wind speed exhibits self-similarity. This means that the wind fields for another synoptic wind speed in the same direction can be obtained through simple scaling. As a result, a set of pre-calculated wind fields for different wind directions can effectively cover all possible scenarios of neutrally stratified atmospheric boundary layer conditions across the domain. Given the high aerodynamic roughness of the urban surface, the role of thermal stratification in the lower part of the atmospheric boundary layer was assumed to be small.

RI-URBANS (www.RIURBANS.eu) is supported by the European Commission under the Horizon 2020 – Research and Innovation Framework Programme, H2020-GD-2020, Grant Agreement number: 101036245

A simulation setup has been developed with the SILAM chemistry-transport model, driven with the wind fields from the pre-calculated set of PALM simulations for the vicinity of the city of Turku at the resolution of 16 m. For every hour of the simulations, a mean wind speed and direction at a blending height over the city of Turku have been evaluated from the forecasts of the Harmonie model. The Harmonie model operates at a resolution of 2.5 km within the Mesoscale Ensemble prediction system over the Fenno-Scandian domain. Then, a corresponding wind direction is selected from the precalculated set of PALM simulations and scaled to the required wind speed. The resulting set of wind-speed fields is used to drive the air-quality setup of the SILAM model. The model receives the emission dataset from a high-resolution inventory developed by Turku, with superimposed temporal profiles used for regional air-quality forecasts. The chemistry boundary conditions are taken from the operational regional SILAM air-quality setup at 2.5 km resolution, driven with the aforementioned Harmonie forecasts.

With this setup steady-state fields of pollutant concentrations for given conditions can be obtained. By repeating these simulations for every hour of the regional-scale Harmonie and SILAM forecast one can obtaina 48-hour forecast of the air pollution in the city at a 16-m resolution.

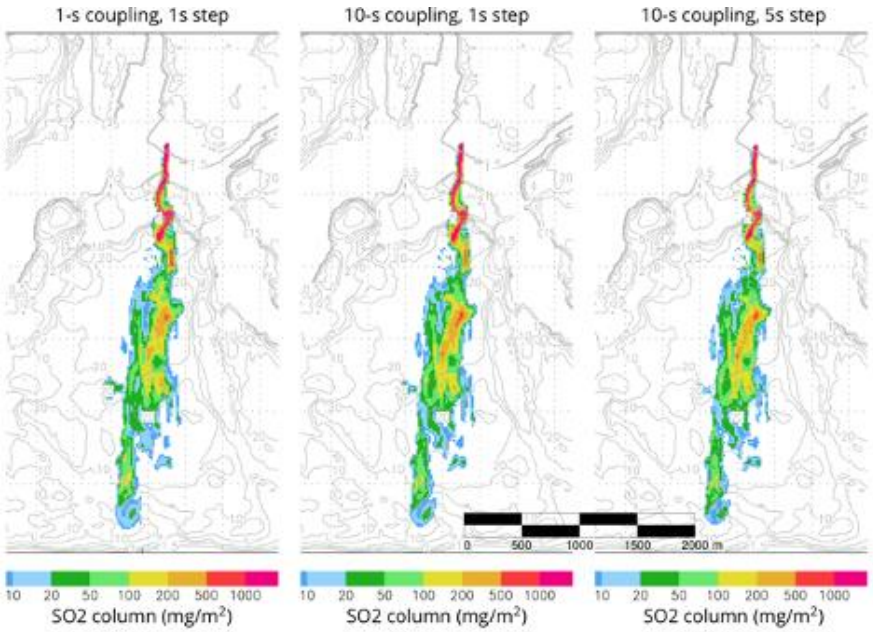

Figure 12. *The SO_2 column resulting from a ship plume in the Turku harbour obtained with the SILAM/PALM model setup. The synoptic wind is from North at a speed of 5 m s^{-1}.*

The setup has been tested with a point-source emissions from a ship in the Turku harbour. The simulations with relatively infrequent coupling between the LES model and SILAM indicated that the size of the wind field dataset needed to generate realistic concentration fields can be relatively small. The plumes generated with 1-second and with 5-second coupling intervals were practically indistinguishable. Besides that, offline simulations of allow for notably longer time step than in the driving LES model (Figure 12).

The prototype setup of SILAM/PALM for air-quality simulations over the city of Turku has been developed. The computations have proven feasible from technical/computational standpoint. An example of resulting concentrations of atmospheric pollution (NO_x) is given in Figure 13.

RI-URBANS (www.RIURBANS.eu) is supported by the European Commission under the Horizon 2020 – Research and Innovation Framework Programme, H2020-GD-2020, Grant Agreement number: 101036245

The setup can be replicated for other locations that have detailed information on local emissions, and work on making a similar setup for Helsinki metropolitan area is going on. The approach can be utilized for studies of chemistry-transport interactions at a deca-meter scales e.g. within street canyons.

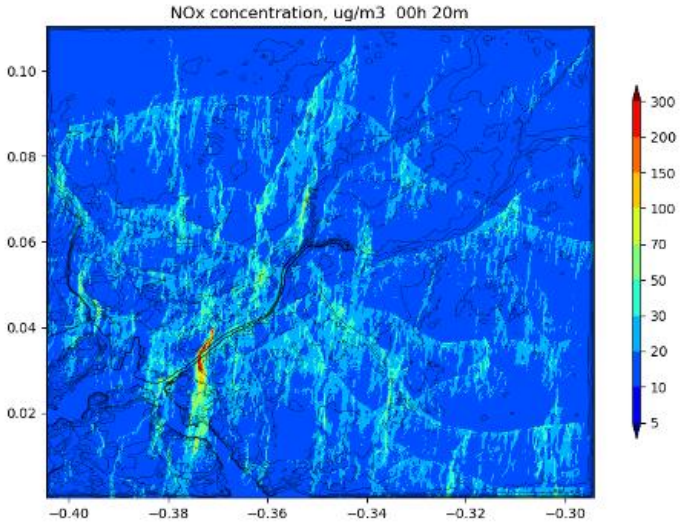

Figure 13. *The near-surface concentrations of NO_x over 12x12 km^2 domain around the city of Turku simulated with SILAM/PALM setup at 16 m resolution. The synoptic wind is from North at a speed of 5 m s^{-1}.*

6. Model toolbox for vertical model evaluation above urban areas

The CAMS European Air Quality (AQ) service products are produced based on forecasts from 11 European models, CHIMERE, DEHM, EMEP, EURAD, GEM-AQ, LOTOS-EUROS, MATCH, MINNI, MOCAGE, MONARCH and SILAM. An ENSEMBLE product is generated from these forecasts and analyses. These models run at a resolution of 0.1 x 0.1 degree for a large European domain, covering the major urban areas with multiple grid cells. Forecast results can be found at https://atmosphere.copernicus.eu/european-air-quality-forecast-plots. At the same time these models produce daily analyses for the past 24 hours by assimilating the available observations. At the moment these analyses are primarily based on hourly surface observations of regulatory species, including NO_2, O_3, PM_{10}, $PM_{2.5}$ and SO_2.

Satellite observations receive growing attention and currently there is an effort within the EU CAMEO development project to develop the assimilation of NO_2 satellite observations of TROPOMI on Sentinel-5P. TROPOMI has a unique resolution of 3.5 x 5 km at nadir, smaller than the grid cell of the regional models. TROPOMI has one single overpass each day with a 13:30 equator crossing time. After the launch of the geostationary Sentinel-4 this observation capability will be extended to hourly observations during daytime.

The validation of these 11 AQ models are also primarily based on surface data, see e.g. Fig. 11. The results from the routine comparisons are public, provided by the operational AeroVal evaluation server, allowing in-depth comparisons between the surface observation, the 11 models and the Ensemble for individual stations and for regional means, see https://cams2-83.aeroval.met.no.

RI-URBANS (www.RIURBANS.eu) is supported by the European Commission under the Horizon 2020 – Research and Innovation Framework Programme, H2020-GD-2020, Grant Agreement number: 101036245

6.1 Routine evaluation of AQ models above the surface

A validation of the models above the surface has been developed in CAMS phase-1 (CAMS-84 contract) and the MACC projects, resulting in a series of quarterly reports. The measurement datasets considered in this activity were:

- O_3 profiles from ozone sonde launches.
- O_3 and CO take-off and landing profiles over airports measured by routine aircraft from the IAGOS research infrastructure.
- Surface remote sensing of NO_2 tropospheric columns/profiles with MAX-DOAS instruments.
- Satellite NO_2 tropospheric column data from GOME-2.
- Satellite CO columns from the MOPITT instrument.
- O_3 and CO in-situ observations at high-altitude (mountain) sites (EEA, GAW), representative for the free troposphere.
- Aerosol lidar extinction profiles from ACTRIS-EARLINET.
- Aerosol Optical Depth observations from the AERONET network.

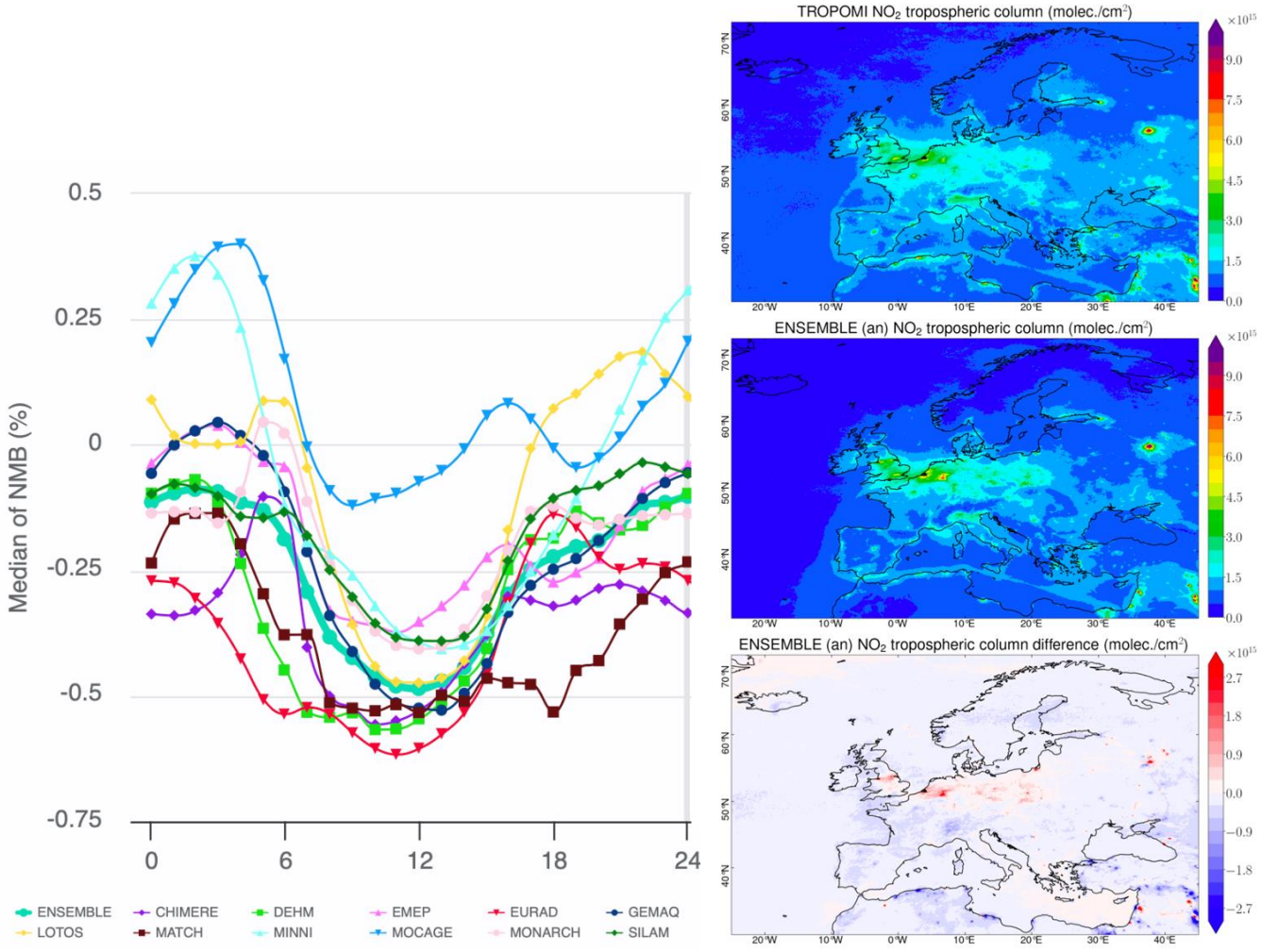

Figure 14. *Left: Normalised mean bias in NO_2 for the 1-day forecasts of the 11 regional air quality models and the CAMS ensemble, against surface observations, averaged over the year 2023. Data taken from https://cams2-83.aeroval.met.no. Right: NO_2 tropospheric columns of TROPOMI (top panel), the ENSEMBLE analysis (middle panel) and the difference between the ENSEMBLE analysis and TROPOMI (bottom panel) during the JJA-2023 period. Unit: 10^{15} molecules/cm^2. Report taken from https://atmosphere.copernicus.eu/regional-services.*

RI-URBANS (www.RIURBANS.eu) is supported by the European Commission under the Horizon 2020 – Research and Innovation Framework Programme, H2020-GD-2020, Grant Agreement number: 101036245

In CAMS phase 2 the CAMS2_83 contract has provided a continuation of part of these above surface comparisons, focussing on:

- Satellite NO_2 tropospheric column data from TROPOMI (Figure 14).
- O_3 profiles from O_3 sounding (Figure 15).
- O_3 and CO take-off and landing profiles over airports measured by routine aircraft from the IAGOS research infrastructure (Figure 15).

The TROPOMI satellite comparisons will be further extended to include HCHO and CHOCHO, now that forecasts for these species are also made available by the models. The reports are available from *https://atmosphere.copernicus.eu/regional-services*.

In recent years the number of PANDORA instruments contributing routine observations to the PANDONIA network, https://www.pandonia-global-network.org, has grown enormously, and has become an important source of information to validate the satellite retrieval products and modelled column amounts, e.g. Verhoelst et al., 2021. Ceilometer instruments, a widespread network in Europe, are also increasingly used for aerosol profile monitoring, see https://e-profile.eu/ or https://vprofiles.met.no/, and are also planned to be used to evaluate the CAMS products. Aircraft column mapping observations for NO_2 are also very valuable to observe the fine-scale variability over urban areas and to understand and validate the satellite observations, e.g. Tack et al. (2021).

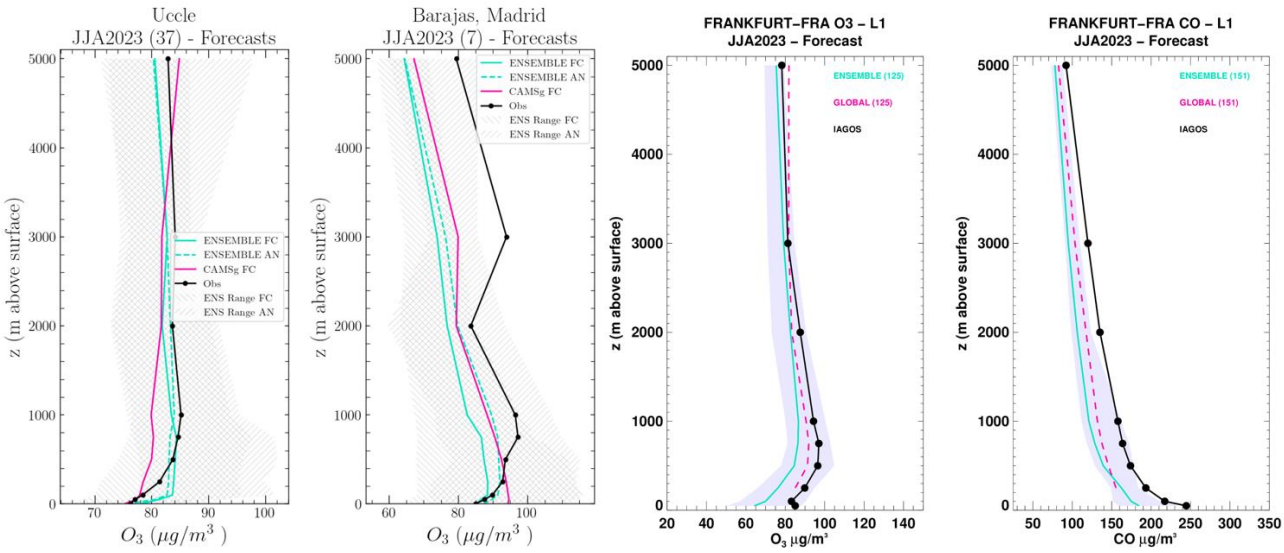

Figure 15. *Left: Comparison between modelled (forecasts) and observed atmospheric ozone concentrations, averaged over the JJA2023 period. The models are the ENSEMBLE and CAMS-global, while 'Obs' (black line) are measurements made by ozone sondes. The hatched line area visualizes the spread among the ENSEMBLE of CAMS regional models (min to max) for the analysis (AN) and the forecast (FC). The numbers in parentheses of each plot indicate the number of sonde launches averaged to produce the profile. Right: Comparison between forecasts and measured atmospheric ozone and CO concentrations at Frankfurt, averaged over the JJA2023 period. The models are the ENSEMBLE and CAMS-global, while 'IAGOS' (black line) are measurements made by aircraft. The shaded area visualizes the spread among the CAMS regional models (min to max). The numbers in parentheses in the legends indicate the number of takeoffs/landings averaged to produce the profile. Report taken from https://atmosphere.copernicus.eu/regional-services.*

RI-URBANS (www.RIURBANS.eu) is supported by the European Commission under the Horizon 2020 – Research and Innovation Framework Programme, H2020-GD-2020, Grant Agreement number: 101036245

6.2 Dedicated campaigns measuring pollution in and above urban areas

In September 2022 a dedicated campaign was held in Rotterdam, The Netherlands, to study the influence of pollution hot-spots. This campaign was organised in the framework of the RI-URBANS T4.5, in collaboration with the Dutch atmospheric research community Ruisdael Observatory. During this campaign, observations were made to augment the permanent ground-based monitoring with several temporary stations including in-situ and remote sensing instruments, mobile observations and airborne observations (in-situ and remote sensing). These data have not been fully analysed yet. An example of preliminary results from the airborne observations is shown in Figure 16.

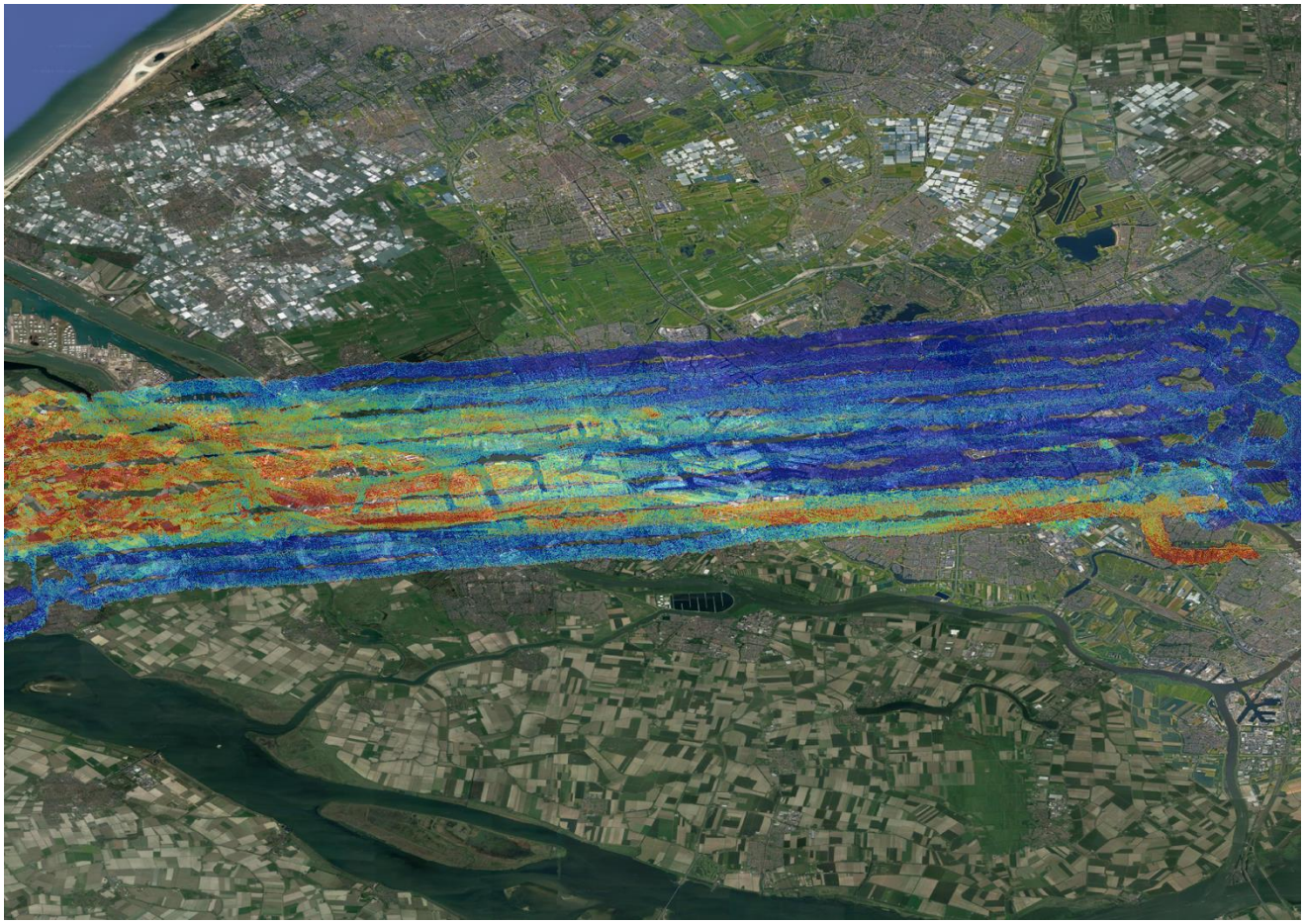

Figure 16. *Example of preliminary NO_2 vertical column densities mapped on 1 September 2022 over the city and harbour of Rotterdam (NL) by airborne remote sensing using the TNO-Spectrolite instrument (Bart Speet), processed by KNMI (Benjamin Leune) and BIRA (Frederik Tack). Blue colours indicate low amounts of NO_2 and red is for higher concentrations. The industrialised area in the West clearly shows higher concentrations than towards the more rural East part in the image.*

6.3 NO_2 in urban areas

Validating models in urban areas is far from trivial. The CAMS models can resolve suburbs from the major (mega-) cities in Europe, but do not resolve the strong gradients in the cities linked to the road networks and industrial activities. Monitoring stations close to major roads will report much higher concentrations than the modelled 0.1 x 0.1 degree grid-box averages. The selection of stations (Joly and Peuch, 2012) which are representative enough to be compared with the CAMS models remains critical. Model downscaling activities to describe the local gradients

RI-URBANS (www.RIURBANS.eu) is supported by the European Commission under the Horizon 2020 – Research and Innovation Framework Programme, H2020-GD-2020, Grant Agreement number: 101036245

in cities, e.g. as described in this report, is another way to facilitate meaningful comparisons with the ground stations.

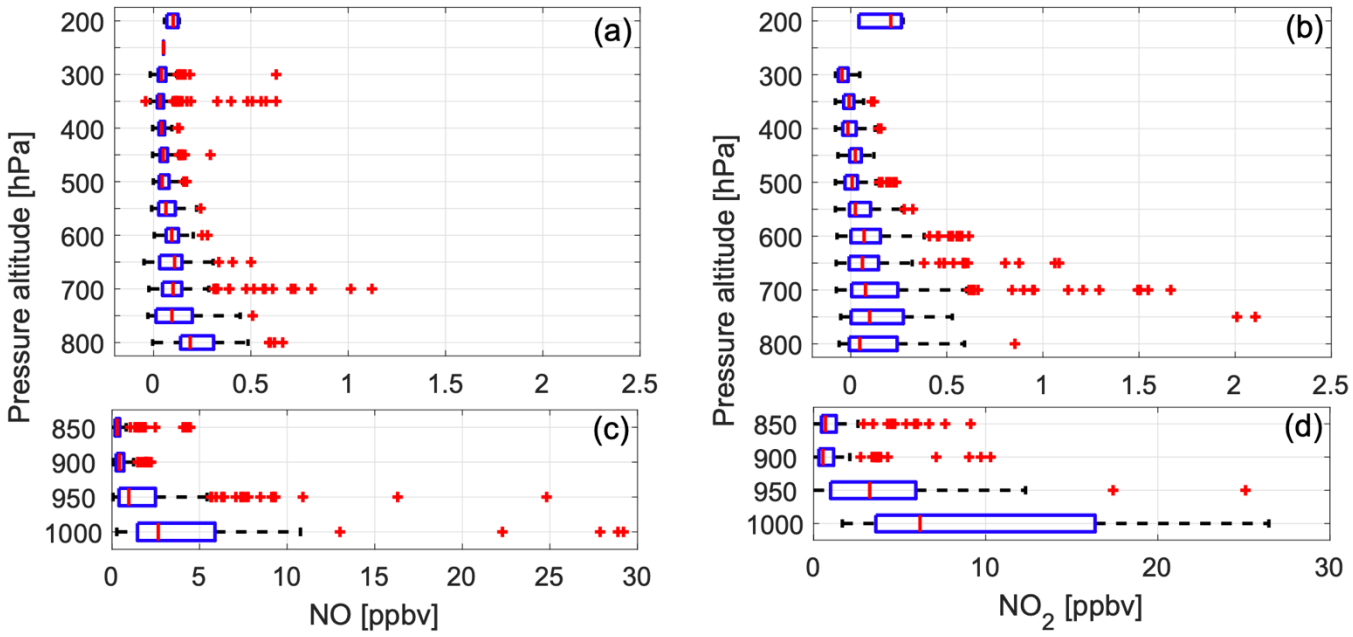

Figure 17. *Statistical vertical distribution of NO and NO_2 (only at daytime) for (a, c) NO and (b, d) NO_2 over Düsseldorf Airport in summer (JJA) 2015. Note the different x-axis scale. Image reproduced from Berkes et al. (2018).*

An important aim of CAMS is to make use of both the surface observations and total column satellite observations of NO_2. The comparison with surface observations of NO_2 in Figure 17 shows a clear negative bias of the models compared to the observations, especially during daytime. Such biases are observed for all seasons. The comparison with the satellites gives a different picture. Here the models show typically higher tropospheric columns in England, Netherlands, Belgium, Germany, Poland, especially in Winter, and somewhat lower columns in the countries below 50N. This shows that meaningful assimilation experiments have to understand and/or correct for these different biases before assimilating both datasets.

There may be several reasons for these biases. The selection of stations, and representativity of stations for model grid cells was already mentioned. Furthermore, the measurement technique used for surface NO_2 is also sensitive to other oxidized nitrogen compounds such as peroxyacetyl nitrate and nitric acid (e.g. Steinbacher et al., 2007). Therefore, NO_2 is overestimated. We note that this effect will normally be less pronounced close to sources, in urban areas, as compared to aged air in rural areas.

Satellite retrievals also have uncertainties. The early TROPOMI product showed a clear low bias compared to surface remote sensing observations (Verhoelst et al., 2021). Later versions of the product (v2.x) showed higher NO_2 columns and better match with independent observations (van Geffen, 2022). A complicating factor in comparisons is the difference in sensitivity profiles between satellite and surface remote sensing. The retrieval uses low-resolution global model profiles of NO_2, with a resolution of 1x1 degree, which leads to low biases in the retrievals over urban areas (Douros et al., 2023). Such biases are avoided when comparisons are made using the averaging kernels of the retrieval. Also, the free tropospheric NO_2 column, which is typically quite uncertain in models, plays a role in the quantitative comparisons (Douros et al., 2023).

RI-URBANS (www.RIURBANS.eu) is supported by the European Commission under the Horizon 2020 – Research and Innovation Framework Programme, H2020-GD-2020, Grant Agreement number: 101036245

Independent profile observations are key information to bridge the gap between the evaluation of surface concentrations and satellite columns. The IAGOS programme includes several aircraft equipped with NOx packages (Figure 17; Berkes et al., 2018). The IAGOS NO_x data is not routinely available yet, but we hope they will become available soon.

6.4 Proposed toolbox for model evaluations over urban areas

As mentioned, the routine validation activity in CAMS is currently based on surface observations of the prime regulatory components (NO_2, O_3, PM_{10}, $PM_{2.5}$ and SO_2), on TROPOMI satellite data of NO_2 (later also HCHO and CHOCHO), on O_3 profiles from sondes and IAGOS, and on CO profile from IAGOS.

The aim of the urban toolbox is threefold:

- To study the added value of above-surface observations which are currently not exploited in an operational way.
- To provide a link between in-situ surface and satellite column observations by using profile observations.
- To exploit campaign data to better understand the three-dimensional distribution of pollutants.

The toolbox will make use of the following observations to evaluate models over urban areas:

- IAGOS NO and NO_2 aircraft observations during take-off and landing (Frankfurt, Paris and other airports when available). These observations will be compared with satellite and in-situ observations.
- PANDORA and MAXDOAS surface remote sensing data, with a focus on NO_2.
- Lidar profiles from EARLINET (ACTRIS) and Ceilometers to study the vertical profiles of aerosol over urban areas, to link surface PM, surface AOD (Aeronet) and satellite aerosol observations.
- Datasets from campaigns with a focus on urban areas (Ruisdael Rotterdam campaign, CINDI-3), using the following observations: TNO-Spectrolite, BIRA-SWING, as well as a suite of ground based in-situ monitors on fixed and mobile platforms.

Experience with these observations and model comparisons will be valuable for future operational validation activities in CAMS.

7. References

AIMSUN: AIMSUN Next, https://www.aimsun.com/aimsun-next/, 2019.

Amato, F., Karanasiou, A., Moreno, T., Alastuey, A., Orza, J. A. G., Lumbreras, J., Borge, R., Boldo, E., Linares, C., Querol, X.: Emission factors from road dust resuspension in a Mediterranean freeway, Atmos. Environ., 61, 580–587, https://doi.org/10.1016/j.atmosenv.2012.07.065, 2012.

Amato, F., Pérez, N., López, M., Ripoll, A., Alastuey, A., Pandolfi, M., Karanasiou, A., Salmatonidis, A., Padoan, E., Frasca, D., Marcoccia, M., Viana, M., Moreno, T., Reche, C., Martins, V., Brines, M., Minguillón, M. C., Ealo, M., Rivas, I., van Drooge, B., Benavides, J., Craviotto, J. M., and Querol, X.: Vertical and horizontal fall-off of black carbon and NO2 within urban blocks, Sci. Total Environ., 686, 236–245, https://doi.org/10.1016/j.scitotenv.2019.05.434, 2019.

Badia, A., Jorba, O., Voulgarakis, A., Dabdub, D., Pérez García-Pando, C., Hilboll, A., Gonçalves, M., and Janjic, Z.: Description and evaluation of the Multiscale Online Nonhydrostatic AtmospheRe CHemistry model (NMMB-MONARCH) version 1.0: gas-phase chemistry at global scale, Geosci. Model Dev., 10, 609–638, https://doi.org/10.5194/gmd-10-609-2017, 2017.

RI-URBANS (www.RIURBANS.eu) is supported by the European Commission under the Horizon 2020 – Research and Innovation Framework Programme, H2020-GD-2020, Grant Agreement number: 101036245

Baldasano, J., Pay, M., Jorba, O., Gassó, S., Jiménez-Guerrero, P.: An annual assessment of air quality with the CALIOPE modeling system over Spain, Sci. Total Environ., 409, 2163–2178, https://doi.org/10.1016/j.scitotenv.2011.01.041, 2011.

Benavides, J.: Development and evaluation of a street-scale air quality modelling system for the city of Barcelona, PhD Thesis, Universitat Politècnica de Catalunya, 2020.

Benavides, J., Snyder, M., Guevara, M., Soret, A., Pérez García-Pando, C., Amato, F., Querol, X., Jorba, O.: CALIOPE-Urban v1.0: coupling R-LINE with a mesoscale air quality modelling system for urban air quality forecasts over Barcelona city (Spain), Geosci. Model Dev., 12, 2811–2835, https://doi.org/10.5194/gmd-12-2811-2019, 2019.

Berkes, F., Houben, N., Bundke, U., Franke, H., Pätz, H.-W., Rohrer, F., Wahner, A., Petzold, A.: The IAGOS NOx instrument – design, operation and first results from deployment aboard passenger aircraft, Atmos. Meas. Tech., 11, 3737–3757, https://doi.org/10.5194/amt-11-3737-2018, 2018.

Bernard, Y., Pniewska, I., Tietge, U., Mock, P., Kodjak, D., Muncrief, R., Watson, S., Dallmann, T., Mahalana, A., Rintanen, I., Narla, A.: TRUE Brussels emissions testing: DPF malfunctions and tampering responsible for 90% of all diesel Euro 5b and 6 emissions. Available at: https://www.trueinitiative.org/blog/2021/may/true-brussels-emissions-testing-dpf-malfunctions-and-tampering-responsible-for-90-of-all-diesel-euro-5b-and-6-emissions (last accessed February 2024), 2021.

Boylan J.W, Russell A.G.: PM and light extinction model performance metrics, goals, and criteria for three-dimensional air quality models, Atmos. Env., 40, 26, 4946-4959, https://doi.org/10.1016/j.atmosenv.2005.09.087, 2006.

Copernicus: State-of-the-European-climate: February 2018, https://surfobs.climate.copernicus.eu/stateoftheclimate/february2018.php, [Online; accessed February 2024], 2018.

Denby, B. R., Sundvor, I., Johansson, C., Pirjola, L., Ketzel, M., Norman, M., Kupiainen, K., Gustafsson, M., Blomqvist, G., Omstedt, G.: A coupled road dust and surface moisture model to predict non-exhaust road traffic induced particle emissions (NORTRIP). Part 1: Road dust loading and suspension modelling, Atmos. Environ., 77, 283-300, https://doi.org/10.1016/j.atmosenv.2013.04.069, 2013.

Douros, J., Eskes, H., van Geffen, J., Boersma, K. F., Compernolle, S., Pinardi, G., Blechschmidt, A.-M., Peuch, V.-H., Colette, A., Veefkind, P.: Comparing Sentinel-5P TROPOMI NO2 column observations with the CAMS regional air quality ensemble, Geosci. Model Dev., 16, 509–534, https://doi.org/10.5194/gmd-16-509-2023, 2023.

Fagerli, H., Tsyro, S., Jonson, J.E., Nyíri, A., Gauss, M., Simpson, D., Wind, P., Benetictow, A., Klein, H., Mortier, A., et al.: Transboundary particulate matter, photo-oxidants, acidifying and eutrophying components, 2019.

Florczyk, A.J., Corbane, C., Ehrlich, D., Freire, S., Kemper, T., Maffenini, L., Melchiorri, M., Pesaresi, M., Politis, P., Schiavina, M., Sabo, F., Zanchetta, L.: GHSL Data Package 2019, EUR 29788EN. Publications Office of the European Union, Luxembourg, https://doi.org/10.2760/062975, 978-92-76-08725-0, JRC117104, 2019.

Giechaskiel, B., Forloni, F., Carriero, M., Baldini, G., Castellano, P., Vermeulen, R., Kontses, D., Fragkiadoulakis, P., Samaras, Z., Fontaras, G.: Effect of Tampering on On-Road and Off-Road Diesel Vehicle Emissions, Sustainability, 14, 6065, https://doi.org/10.3390/su14106065, 2022.

Guevara, M., Tena, C., Porquet, M., Jorba, O., Pérez García-Pando, C.: HERMESv3, a stand-alone multiscale atmospheric emission modelling framework – Part 2: The bottom–up module, Geosci. Model Dev., 13, 873–903, https://doi.org/10.5194/gmd-13-873-2020, 2020

RI-URBANS (www.RIURBANS.eu) is supported by the European Commission under the Horizon 2020 – Research and Innovation Framework Programme, H2020-GD-2020, Grant Agreement number: 101036245

Guevara, M., Jorba, O., Tena, C., Denier van der Gon, H., Kuenen, J., Elguindi, N., Darras, S., Granier, C., Pérez García-Pando, C.: Copernicus Atmosphere Monitoring Service TEMPOral profiles (CAMS-TEMPO): global and European emission temporal profile maps for atmospheric chemistry modelling, Earth Syst. Sci. Data, 13, 367–404, https://doi.org/10.5194/essd-13-367-2021, 2021.

Hausberger, S., Rexeis, M., Zallinger, M., Luz, R.: Emission Factors from the Model PHEM for the HBEFA Version 3, Tech. rep., Institute for Internal Combustion Engines and Thermodynamics. Technische Universität Graz (TUG), Graz, Austria, https://assets.website-files.com/6207922a2acc01004530a67e/625e7fbf0ee7ac6fc3e12fbd_HBEFA_31_Docu_hot_emissionfactors_PC_LCV_HDV.pdf, 2009.

Joly, M., Peuchm V.-H., Objective classification of air quality monitoring sites over Europe, Atmos. Environ., 47, 111-123, https://doi.org/10.1016/j.atmosenv.2011.11.025, 2012.

Järvi, L., Kuuluvainen, H., Rönkkö, T., Karttunen, S., Balling, A., Timonen, H., Niemi, J. V., Pirjola, L.: Determinants of spatial variability of air pollutant concentrations in a street canyon network measured using a mobile laboratory and a drone, Sci. Total Environ., 856, 158–974, https://doi.org/10.1016/j.scitotenv.2022.158974, 2023.

Lugon L, Sartelet K, Kim Y, Vigneron J, Chrétien O: Simulations of primary and secondary particles in the streets of Paris using MUNICH, Faraday Discussions, http://dx.doi.org/10.1039/D0FD00092B, 2021.

Kim, Y., Lugon, L., Maison, A., Sarica, T., Roustan, Y., Valari, M., Zhang, Y., André, M., Sartelet, K.: MUNICH v2.0: a street-network model coupled with SSH-aerosol (v1.2) for multi-pollutant modelling, Geosci. Model Dev., 15, 7371–7396, https://doi.org/10.5194/gmd-15-7371-2022, 2022.

Kurppa, M., Hellsten, A., Roldin, P., Kokkola, H., Tonttila, J., Auvinen, M., Kent, C., Kumar, P., Maronga, B., Järvi, L.: Implementation of the sectional aerosol module SALSA2.0 into the PALM model system 6.0: model development and first evaluation, Geosci. Model Dev., 12, 1403–1422, https://doi.org/10.5194/gmd-12-1403-2019, 2019.

Maronga, B., Banzhaf, S., Burmeister, C., Esch, T., Forkel, R., Fröhlich, D., Fuka, V., Gehrke, K. F., Geletič, J., Giersch, S., et al.: Overview of the PALM model system 6.0, Geosci. Model Dev., 13, 1335–1372, https://doi.org/10.5194/gmd-13-1335-2020, 2020.

Menut, L., Bessagnet, B., Briant, R., Cholakian, A., Couvidat, F., Mailler, S., Pennel, R., Siour, G., Tuccella, P., Turquety, S., Valari, M.: The chimere v2020r1 online chemistry-transport model, Geosci. Model Dev., 14(11):6781–6811, https://doi.org/10.5194/gmd-14-6781-2021, 2021

Navarro-Barboza, H., Pandolfi, M., Guevara, M., Enciso, S., Tena, C., Via, M., Yus-Díez, J., Reche, C., Pérez, N., Alastuey, A., Querol, X., Jorba, O.: Uncertainties in source allocation of carbonaceous aerosols in a Mediterranean region, Environ. Int., 183, 108252, https://doi.org/10.1016/j.envint.2023.108252, 2024.

Ntziachristos, L., Boulter, P.: Road vehicle tyre and brake wear. Road surface wear. Joint EMEP/CORINAIR emission inventory guidebook, permalink: 35a310a433014118ab2cb6b0f7d77422, 2023.

Petzold, A., Schönlinner, M.: Multi-angle absorption photometry—a new method for the measurement of aerosol light absorption and atmospheric black carbon, J. Aerosol Sci. 35, 421–441, https://doi.org/10.1016/j.jaerosci.2003.09.005, 2004.

Rodríguez-Rey, D., Guevara, M., Linares, M.P., Casanovas, J., Salmerón, J., Soret, A., Jorba, O., Tena, C., Pérez García-Pando, C.: A coupled macroscopic traffic and pollutant emission modelling system for Barcelona, Transportation Research Part D, 92, 102725, https://doi.org/10.1016/j.trd.2021.102725, 2021.

RI-URBANS (www.RIURBANS.eu) is supported by the European Commission under the Horizon 2020 – Research and Innovation Framework Programme, H2020-GD-2020, Grant Agreement number: 101036245

Roldin, P., Swietlicki, E., Schurgers, G., Arneth, A., Lehtinen, K. E. J., Boy, M., Kulmala, M.: Development and evaluation of the aerosol dynamics and gas phase chemistry model ADCHEM, Atmos. Chem. Phys., 11, 5867–5896, https://doi.org/10.5194/acp-11-5867-2011, 2011.

Sandradewi, J., Prevot, A.S., Szidat, S., Perron, N., Alfarra, M.R., Lanz, V.A., Weingartner, E., Baltensperger, U.: Using aerosol light absorption measurements for the quantitative determination of wood burning and traffic emission contributions to particulate matter, Environ. Sci. Technol. 42, 3316–3323, https://doi.org/10.1021/es702253m, 2008.

Sartelet, K., Couvidat, F., Wang, Z., Flageul, C., Kim, Y.: SSH-Aerosol v1.1: A Modular Box Model to Simulate the Evolution of Primary and Secondary Aerosols, Atmosphere, 11, 525, https://doi.org/10.3390/atmos11050525, 2020.

Sartelet, K., Kim, Y., Couvidat, F., Merkel, M., Petäjä T., Sciare J., Wiedensohler, A.: Influence of emission size distribution and nucleation on number concentrations over Greater Paris, Atmos, Chem. Phys., 22, 8579-8596, https://doi.org/10.5194/acp-22-8579-2022, 2022.

Savadhooki, M., Pandolfi, M., Reche, C., Niemi, J., Mooibroek, D., Titos, G., Green, D., Tremper, A., Hueglin, C., Liakakou, E., et al.: The variability of mass concentrations and source apportionment analysis of equivalent black carbon across urban Europe, Environ. Int., 178:108081, https://doi.org/10.1016/j.envint.2023.108081, 2023.

Steinbacher, M., Zellweger, C., Schwarzenbach, B., Bugmann, S., Buchmann, B., Ordóñez, C., Prevot, A.S.H., Hueglin, C.: Nitrogen oxide measurements at rural sites in Switzerland: Bias of conventional measurement techniques, J. Geophys. Res., 112, D11307, https://doi.org/10.1029/2006JD007971, 2007

Strömberg, J., Li, X., Kurppa, M., Kuuluvainen, H., Pirjola, L., Järvi, L.: Effect of radiation interaction and aerosol processes on ventilation and aerosol concentrations in a real urban neighbourhood in Helsinki, Atmos. Chem. Phys., 23, 9347–9364, https://doi.org/10.5194/acp-23-9347-2023, 2023.

Tack, F., Merlaud, A., Iordache, M.-D., Pinardi, G., Dimitropoulou, E., Eskes, H., Bomans, B., Veefkind, P., Van Roozendael, M.: Assessment of the TROPOMI tropospheric NO2 product based on airborne APEX observations, Atmos. Meas. Tech., 14, 615–646, https://doi.org/10.5194/amt-14-615-2021, 2021.

Tong, Z., Wang, Y. J., Patel, M., Kinney, P., Chrillrud, S., Max Zhang, K.: Modeling Spatial Variations of Black Carbon Particles in an Urban Highway-Building Environment, Environ. Sci. Tech., 46, 312–319, https://doi.org/10.1021/es201938v, 2012.

TUG: PHEMlight. User Guide for Version 1, Tech. rep., Technische Universitat Graz, 2017.

Verhoelst, T., Compernolle, S., Pinardi, G., Lambert, J.-C., Eskes, H. J., Eichmann, K.-U., Fjæraa, A. M., Granville, J., Niemeijer, S., Cede, A., et al.: Ground-based validation of the Copernicus Sentinel-5P TROPOMI NO2 measurements with the NDACC ZSL-DOAS, MAX-DOAS and Pandonia global networks, Atmos. Meas. Tech., 14, 481–510, https://doi.org/10.5194/amt-14-481-2021, 2021.

van Geffen, J., Eskes, H., Compernolle, S., Pinardi, G., Verhoelst, T., Lambert, J.-C., Sneep, M., ter Linden, M., Ludewig, A., Boersma, K. F., and Veefkind, J. P.: Sentinel-5P TROPOMI NO2 retrieval: impact of version v2.2 improvements and comparisons with OMI and ground-based data, Atmos. Meas. Tech., 15, 2037–2060, https://doi.org/10.5194/amt-15-2037-2022, 2022.

Yus-Díez, J., Via, M., Alastuey, A., Karanasiou, A., Minguillón, M.C., Perez, N., Querol, X., Reche, C., Ivancic, M., Rigler, M., et al.: Absorption enhancement of black carbon particles in a Mediterranean city and countryside: effect of

RI-URBANS (www.RIURBANS.eu) is supported by the European Commission under the Horizon 2020 – Research and Innovation Framework Programme, H2020-GD-2020, Grant Agreement number: 101036245

particulate matter chemistry, ageing and trend analysis, Atmos. Chem. Phys. 22, 8439–8456, https://doi.org/10.5194/acp-22-8439-2022, 2022.

RI-URBANS (www.RIURBANS.eu) is supported by the European Commission under the Horizon 2020 – Research and Innovation Framework Programme, H2020-GD-2020, Grant Agreement number: 101036245